

Available online at [www.sciencedirect.com](http://www.sciencedirect.com)

ScienceDirect

journal homepage: [www.elsevier.com/locate/he](http://www.elsevier.com/locate/he)

# A Techno-Economic Analysis of solar hydrogen production by electrolysis in the north of Chile and the case of exportation from Atacama Desert to Japan

Felipe Ignacio Gallardo <sup>a</sup>, Andrea Monforti Ferrario <sup>b,c,\*</sup>, Mario Lamagna <sup>d</sup>, Enrico Bocci <sup>b</sup>, Davide Astiaso Garcia <sup>e</sup>, Tomas E. Baeza-Jeria <sup>f</sup>

<sup>a</sup> H2Chile Chilean Hydrogen Association, Santiago, Chile

<sup>b</sup> Department of Nuclear, Subnuclear and Radiation Physics, Università degli Studi Guglielmo Marconi, Via Plinio 44, Rome, Italy

<sup>c</sup> Centro Interuniversitario di Ricerca Per lo Sviluppo Sostenibile “CIRPS”, Piazza U. Pilozzi, Valmontone, Italy

<sup>d</sup> Department of Astronautics, Electric and Energy Engineering, Sapienza University of Rome, Via Eudossiana 18, Italy

<sup>e</sup> Department of Planning, Design, and Technology of Architecture, Sapienza University of Rome, Via Flaminia 72, Rome, Italy

<sup>f</sup> Chilean Solar and Energy Innovation Committee, Agustinas 640, Santiago, Chile

## HIGHLIGHTS

- Cost-competitive solar hydrogen can be produced in Chile.
- Oversized PV-supplied systems lead to lower LCOH than smaller CSP-supplied systems.
- The LCOH of PV-PPA+ALK can reach 2.20 US\$/kg in 2018 and 1.67 US\$/kg in 2025.
- Storage and transport phases are CAPEX intensive, favoured by flat supply schemes.
- Competitive H<sub>2</sub> can be delivered in Japan in 2018 and 2025 respect to target prices.

## ARTICLE INFO

### Article history:

Received 13 March 2020

Received in revised form

26 May 2020

Accepted 6 July 2020

Available online 1 August 2020

### Keywords:

Solar hydrogen

Techno-Economic Analysis

## ABSTRACT

H<sub>2</sub> production from solar electricity in the region of the Atacama Desert – Chile – has been identified as strategical for global hydrogen exportation. In this study the full supply chain of solar hydrogen has been investigated for 2018 and projected to scenarios for 2025–2030. Multi-year hourly electrical profiles data have been used from real operating PV plants and simulated Concentrated Solar Power “CSP” plants with Thermal Energy Storage “TES” as well as commercial electricity Power Purchase Agreement “PPA” prices reported in the Chilean electricity market were considered. The Levelized Cost of Hydrogen “LCOH” of each production pathway is calculated by a case-sensitive techno-economic MATLAB/Simulink model for utility scale (multi-MW) alkaline and PEM electrolyser technologies. Successively, different distribution, storage and transportation configurations are evaluated based on the 2025 Japanese case study according to the declared H<sub>2</sub> demand. Transport in the

\* Corresponding author. Department of Nuclear, Subnuclear and Radiation Physics, Università degli Studi Guglielmo Marconi, Via Plinio 44, Rome, Italy.

E-mail address: [a.monforti@lab.unimarconi.it](mailto:a.monforti@lab.unimarconi.it) (A. Monforti Ferrario).

<https://doi.org/10.1016/j.ijhydene.2020.07.050>

0360-3199/© 2020 The Authors. Published by Elsevier Ltd on behalf of Hydrogen Energy Publications LLC. This is an open access article under the CC BY license (<http://creativecommons.org/licenses/by/4.0/>).

form of liquefied hydrogen (LH<sub>2</sub>) and via ammonia (NH<sub>3</sub>) carrier is compared from the port of Antofagasta, CL to the port of Osaka, JP.

© 2020 The Authors. Published by Elsevier Ltd on behalf of Hydrogen Energy Publications LLC. This is an open access article under the CC BY license (<http://creativecommons.org/licenses/by/4.0/>).

## Introduction

### *Solar hydrogen for large-scale exportation - current state of the art*

It has been acknowledged that hydrogen will play a key role in the future energy system worldwide constituting a pillar of the pathway towards energy transformation and in order to reach decarbonization targets [1]. In an increasing trend of variable and intermittent Renewable Energy Sources “RES” [2], the conversion of electricity to H<sub>2</sub> represents a viable pathway to reduce the impacts of renewable electricity on the electricity grids [3]. Moreover, hydrogen enables the integration of renewable electricity in hard to electrify sectors such as heat and industry [4–7] other than providing energy storage capacity, showing competitiveness respect to other technologies for reliability issues or bulk storage [8–10] allowing the exploitation of renewable electricity sparsely produced to be used for end uses elsewhere in a worldwide perspective [8,11–15]. For this reason it is necessary to clearly define and analyse the different pathways of the hydrogen supply chain structure and taxonomy [16].

Techno-economic feasibility of green hydrogen production is highly dependent from country-specific resources and energy market characteristics, which play a key role in determining cost competitiveness. The balance between specific CAPEX (MUS\$/MW), capacity factor (%) and electricity cost (US\$/MWh) is not straightforward and can foster one supply-chain configuration respect to others [8,17]. Also demand volume (ton<sub>H2</sub>/year) deeply affects the cost structure (OPEX or CAPEX-dominated) of the hydrogen supply chain, enabling or inhibiting different hydrogen carrier and logistics concepts [7,9,14,18,19].

Large scale capacity scenarios such as exportation (with hydrogen demands in the order of kton<sub>H2</sub>/year) are favoured by economy of scale. However, investment costs of multi-MW scale electrolysis systems are reportedly hard to determine correctly [20], due to the lack of real cost data references given by the intrinsic upper limit of 1–2 MW of the currently developed stack modules and the few multi-MW projects currently deployed [4,5]; cost estimation and projection must be done carefully to obtain realistic values [20–22].

The transport route, mode and carrier significantly affect the overall supply chain structure and the delivered LCOH. Each step can be extremely complex to model [23–25]. For example Liquefied Hydrogen “LH<sub>2</sub>” presents a mass density which is approximately 700 times the one of Compressed Gaseous Hydrogen “CGH<sub>2</sub>” [26] but the LH<sub>2</sub> transport conditions are by far more challenging [26,27]. Alternative chemical carriers such as ammonia (NH<sub>3</sub>) can be suitable for long-haul

transport, in virtue of the increased mass density of hydrogen and stability at milder operating conditions [9,18,19,25,28]. The coupling of variable renewable energy to LH<sub>2</sub> or NH<sub>3</sub> plants is challenging since such systems are usually operated in steady state [24,29]. For example, several studies have shown the dependency of the conversion cost of NH<sub>3</sub> with the flexibility capability of the considered plants, deeply affecting their operation criteria and the requirements of buffer storage systems [25,30].

Amongst the plethora of possible international trading routes, those which link coastal strategic H<sub>2</sub> producers such as Chile (Atacama Region), Argentina (Patagonia Region), Australia, North Africa (Morocco, Algeria), Middle East (Saudi Arabia, Iran) and coastal strategic H<sub>2</sub> importers such as Japan, USA (California), Northern Europe and Korea stand out [8,11–15,31]. An object of several studies is the route connecting Australia to Japan, considered the main benchmark for Asia-Pacific H<sub>2</sub> trade [8,11–13,31] with a LCOH between 5–7 US\$/kg<sub>H2</sub> delivered in Japan in 2025–2030.

Chile is identified amongst the key strategical countries for H<sub>2</sub> production [8] thanks to the availability of low cost solar electricity: the Atacama Desert of Chile presents one of the highest global horizontal irradiation values in the world equal to more than 2 kWh/m<sup>2</sup> [32] with capacity factors beyond 30% for PV [33] which has experienced a dramatic growth in its installed capacity the last years, reaching 2.14 GW by the end of 2018 [34–37] with reported bids in electricity auctions as low as 21 US\$/MWh [25,38,39] in 2017. The Atacama desert is also extremely promising for CSP plants, which can reach capacity factors beyond 80–85% [33] with estimated Levelised Cost of Electricity “LCOE” of 55 US\$/MWh at utility scale [25,38,39]. Such extremely low cost electricity can be competitively implemented for solar-driven electrolysis as an opportunity to increase the penetration of the abundant, economic and sustainable solar energy in the national energy matrix through solar fuels – particularly solar-hydrogen – both as domestic energy vector and for bulk exportation to other countries. In the Chilean National Long Term Energy Policy [40], which was launched in 2018 by the Ministry of Energy, hydrogen is acknowledged as an innovative technology; in the Solar Energy Program – launched in 2016 by CORFO [41] – business opportunities have been identified for the Atacama and Antofagasta Regions in the North of Chile. The main strategical sectors considered in the short term innovation strategy are mining, chemical and energy sectors while exportation is mentioned as long term strategy [25,39,42–44].

On the other hand, Japan is considered a key hydrogen user, leading the H<sub>2</sub> market worldwide, with over 100 Hydrogen Refueling Stations and more than 3600 Fuel Cell vehicles; more than 300,000  $\mu$ -CHP Fuel Cell units are deployed

in households and several large scale Power-to-Gas and H<sub>2</sub>-based CHP projects are being deployed [45,46]. The Japanese Ministry of Economy, Trade and Industry (METI) have declared a hydrogen demand of 300 kton/year in 2030, including international import, defining a target price of 3 US\$/kg<sub>H2</sub> [12,47] for that year. Currently the retail price of H<sub>2</sub> in Japan is around 10 US\$/kg<sub>H2</sub> [46]. Green H<sub>2</sub> is expected to provide the baseload energy previously supplied by nuclear power plants, following the nuclear shut-down policy, together with other renewable technologies [46]. With regards to the imported share, the first generation LH<sub>2</sub> carrier ships (170 ton<sub>H2</sub>/ship) are currently being developed based on LNG ships. In 2030 a substantial ship capacity ramp-up is foreseen (up to 6.5–11 kton<sub>H2</sub>/ship) [48]. This is expected to pave the way for large-scale maritime hydrogen transport.

Several studies have assessed the feasibility of green hydrogen production [1,8,9,11,12,15,17,31,39,43,49,50]. Global energy outlooks provide useful information and assumptions but they assess H<sub>2</sub> production with an aggregated approach, lacking of specific modelling details [1,8,12,17,39,43,49,50]. Other studies provide detailed information regarding one step of the supply chain such as electrolysis [20,21], ammonia conversion [28] or transport & distribution phases [31,51] without envisaging the full supply chain from a comprehensive point of view. Model-based studies considering real operational data are available [13,19,25,28], although many of them focus on small-scale systems and none considers the full supply chain. Analyses based on Chile have been performed [8,25,39,43,44] although most of them focus on the determination of the production cost from PV and do not fully assess the storage distribution and transport phase with both LH<sub>2</sub> and NH<sub>3</sub>. Only Tractebel [39] has analysed also CSP, comparing direct and PPA electricity supplies by PV and CSP, however the transport phase is not assessed. Also Armijo and Philibert [25] present a detailed model-based analysis for production of electrolytic ammonia in Chile and Argentina but does not assess the subsequent distribution and transport phases, whereas Heuser et al [15] present a full study from production in Chile to delivery for LH<sub>2</sub> in Japan without comparing it to other transport vectors. For this reason, the present study aims to perform a comprehensive Techno-Economic Analysis of the complete supply chain of hydrogen exportation from solar-driven electrolysis in Chile up to the distribution, storage and transportation to Japan via LH<sub>2</sub> or NH<sub>3</sub> carrier with a model-based approach, considering real operating data from solar plants or simulated hourly profiles. Founding a Techno-Economic Analysis on real operating data can provide meaningful information respect to the actual operating conditions and specific constraints, in function of the available instantaneous power profile which affects all the phases of the H<sub>2</sub> supply chain. Such approach can support policy-makers to set suitable targets to enable technology breakthroughs [17,50], or to determine financial support required in order to bridge the gap to competitiveness and foster technology uptake [52].

### Chilean solar energy market

Given the structure of the Chilean electricity market, several alternatives of solar energy generation technologies, energy

supply setups and purchase mechanisms can be assessed. Two types of solar technologies are studied: solar PV, able to provide electricity during solar hours only and CSP + TES, able to provide electricity 24/7 thanks to the TES system. This choice is made based on the well-known market maturity and dominance of PV during solar hours and CSP + TES for 24/7 schemes [53,54]. Solar PV with batteries and CSP without TES options are therefore excluded.

For each technology (PV and CSP+TES) two possibilities have been considered: (i) direct connection with a dedicated plant or (ii) indirect on-grid connection via so called “solar PPA” mechanism, which is a bilateral financial energy contract (Power Purchase Agreements “PPA”) between producers and consumers available in the Chilean electricity market, which secure the supply of power for a settled duration (usually long-term, around 15–20 years) at a fixed nominal power  $P_n$  and electricity price [55–59]. Each scenario defines an energy hourly power supply profile (percentage  $P/P_n$ , each hour) – physical or set by contract – and a respective electricity price level (US\$/MWh). The direct connection is linked to the instantaneous variations of the solar resource; its price equals LCOE of the PV system [25,36,39,56,60,61]. Instead, a solar PPA based on PV technology ensures constant supply at the agreed nominal power during “solar hours” (08–18h), while a Solar PPA based on CSP ensures a constant supply at the agreed nominal power [57,59,62]. The supply by PPA mechanisms is constant throughout the year and do not consider neither daily nor seasonal variations. In this way it is possible to decouple the solar plant respect to the hydrogen plant and avoid variability since the power supply is not directly linked to the physical production. The PPA price is bilaterally negotiated between the producer and the consumer. The PPA scheme is also the base for the public energy auctions within the Chilean market with the distinction that the consumers are the regulated customers subject to distribution grids instead of private customers and the price and terms are not bilaterally negotiated but awarded through a tender process [63,64]. Therefore, a good benchmark for the bilateral PPA pricing are the public auctions results [57,59,62]. The PPA prices are strongly driven by LCOE in function of CAPEX, OPEX and demands volume. Additional markup is applied by generation companies, respect to the direct connection scheme in relation to the risk of mismatches of energy flows and spot price between the physical generation at the injection node (variable) and the supply of demand at the withdraw node (constant) for both daily and seasonal variability [65]. Thus, a solar PPA will be in general, more expensive than the respective LCOE of an onsite dedicated plant for the same energy volume, however the PPA option offers increased reliability due to its constant energy output [57,59,62].

### Solar hydrogen Production

The production of H<sub>2</sub> is studied in 8 different solar hydrogen technology/energy supply coupling configurations (see [Chilean solar energy market section](#)). The chosen electrolysis technologies are Alkaline “ALK” and Proton Exchange Membrane “PEM” due to their commercial maturity (see [Water electrolysis section](#)).

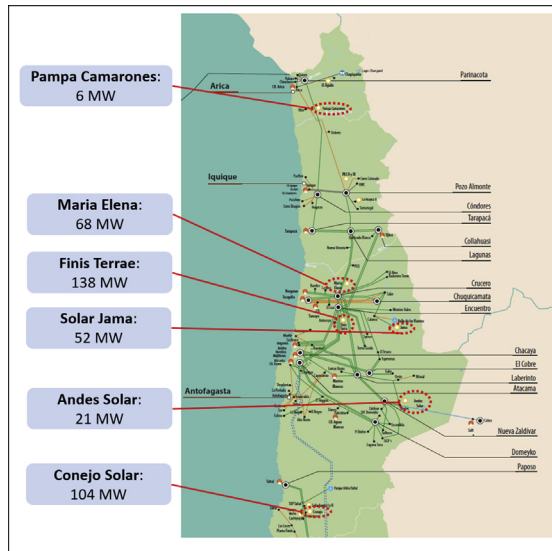


**Fig. 1 – Northern Section of the National Electrical System of Chile "SEN".** Own elaboration based on [67,68].

1. ALK electrolysis, directly supplied by a PV power plant;
2. ALK electrolysis, supplied by a solar PPA (PV);
3. ALK electrolysis, directly supplied by a CSP power plant;
4. ALK electrolysis, supplied by a solar PPA (CSP);
5. PEM electrolysis, directly supplied by a PV power plant;

6. PEM electrolysis, supplied by a solar PPA (PV);
7. PEM electrolysis, directly supplied by a CSP power plant;
8. PEM electrolysis, supplied by a solar PPA (CSP)

In the following subsection A, the input data are presented. The datasets are fed into the  $H_2$  production model developed in MATLAB/Simulink environment as described in subsection B.

### Input data

The operational data for the 6 selected PV plants (Fig. 1) in the Atacama Desert region - Chile, summing up to approximately 400 MW<sub>p</sub> installed, ranging from 6.2 MW<sub>p</sub> to 138 MW<sub>p</sub> per plant [66] are obtained from the national Independent System Operator's (Coordinador Eléctrico Nacional, CEN) public database [34] for 2017. Such public database collects real operational data with hourly resolution. By performing a statistical analysis, the average seasonal electrical profile of a typical solar PV plant in the Atacama Region was obtained.

These 6 PV power plants were selected as reference because they were, at the moment of this study, the only 6 utility-scale PV plants operating in the Atacama Desert, that presented simultaneously two characteristics: (i) hourly data available for at least one year and (ii) at least one continuous year of operation without being subject to transmission congestions or curtailment. Thus, the selected PV plants, offered real output data without being distorted by commercial or electrical transmission constraints, therefore reflecting the

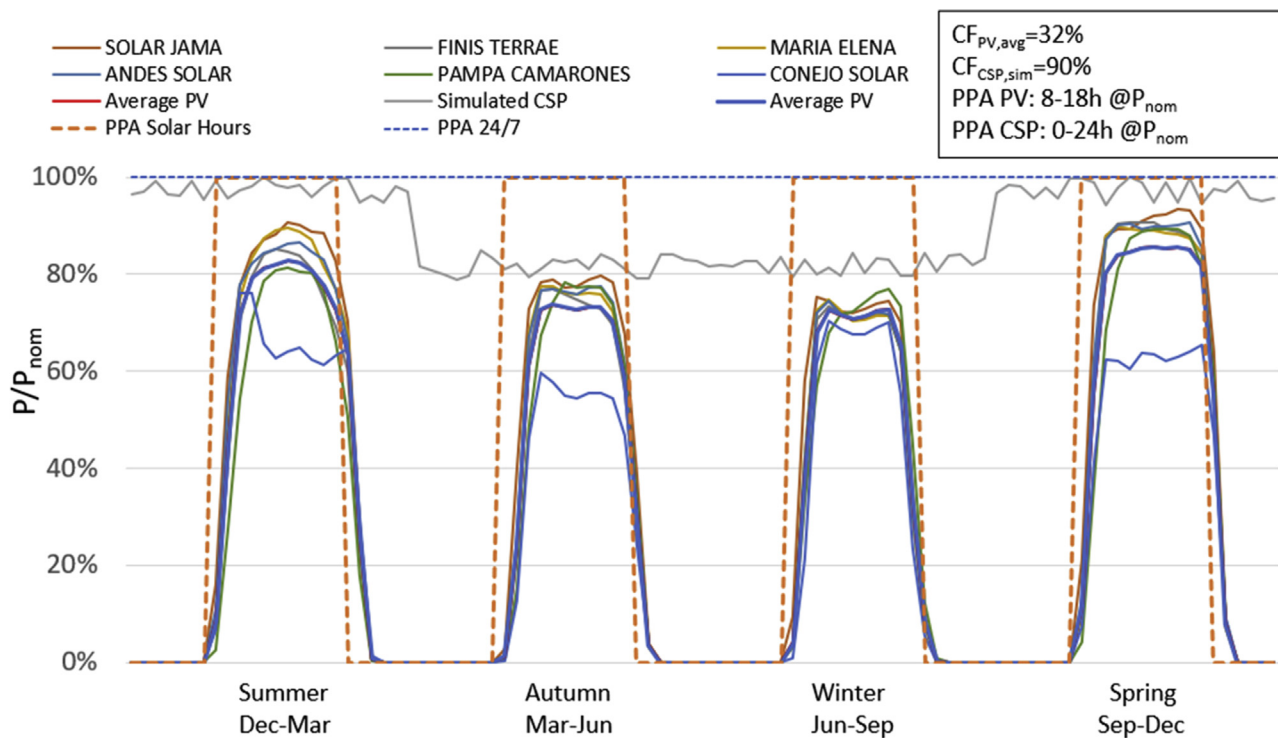


**Fig. 2 – Average seasonal solar electricity profiles (PV and CSP + TES).** Source: Elaboration of CEN Chile (ISO) [34], SAM NREL [69], PPA profiles [57,59,62]



**Table 1 – Electricity prices considered [25,36–39,56,60–62,71–80].**

Supply scheme	2018 (US\$/MWh)	2025 (US\$/MWh)
LCOE Solar PV	21	18
Solar PPA (8–18h, PV based)	23	20
LCOE CSP + TES	55	50
Solar PPA (24/7, CSP + TES based)	63	54

real physical availability of an onsite PV plant in the Atacama Desert.

The CSP + TES (solar tower configuration) operational data – due to the lack of utility scale plants in operation for electricity production in the region [66] – was simulated using NREL System Advisor Model<sup>1</sup> [69] considering an adapted TMY P-50 obtained from PV-GIS databases [70] which consider statistical analysis of 20 year historical meteorological data integrated with ground measured data.

The average seasonal electrical profiles are represented in Fig. 2 and successively fed to the H<sub>2</sub> production model.

The electrical profiles of the two technologies (PV and CSP) differ greatly in the capacity factor, ranging from around 32% for intermittent solar PV against around 89% for CSP + TES, which is stabilized by the thermal storage and whose variations are only due to seasonal variations, as shown in Fig. 2. The capacity factors – obtained from real operating data [34] – are in line with relevant literature references [25,39]. On the other hand, the PPA profiles present greater capacity factors respect to the direct connection ones; up to 41% for PV based solar PPAs (8–18h) and 100% for 24/7 PPAs based on CSP systems, due to the constant power supply ensured within the PPA timeframe.

Table 1 reports the considered electricity cost in all energy supply scenarios for 2018 and their projections to 2025.

For the onsite dedicated PV field, the price of the energy is estimated equal to the LCOE of the system, which is estimated equal to 21 US\$/MWh in 2018 in line with estimations of IRENA for Chile, indicating a range between 16–30 US\$/MWh [60] and with other specific works related to Chile [36,61]. The LCOE for utility scale (>100 MW<sub>e</sub>) CSP + TES (solar tower configuration) in 2018 is estimated by Benitez et al [71] at 55 US\$/MWh based on the 110 MW<sub>e</sub> scale CSP solar tower configuration plant Cerro Dominador plant under construction, located in Atacama Desert in Chile [36,37,61]. The LCOE is aligned with specific works by Gallardo et al. [37], and Comité Solar [61] which report between 60–70 US\$/MWh for the same plant in different operating conditions. NREL [72] reports 60 US\$/MWh as reference for utility scale CSP, therefore a cost reduction is justifiable for the increased solar resource in Chile. For the PPA alternative, the PPA pricing in 2018 has been estimated based on real price offers reported in the national Chilean electricity market (regulated customers) for utility scale, long-term (20 years) PPA-based public auctions in 2017 [25,38,62,73–78]

since bilateral PPA pricing is confidential. Minimum PV-based solar PPAs (8–18h) bids range between 21–25 US\$/MWh [25,38,62,73–75], while reported bids for CSP-based solar PPAs (24/7) are around 60 US\$/MWh [76–78] for two different projects – although bids as low as 48 US\$/MWh have been presented [36,77]. Cost reporting for CSP-based PPA is not simple since the bids were not awarded due to more competitive offers from PV systems which compete in the same auction mechanism [36].

To obtain energy costs in 2025, projected cost reductions by technology were applied to the costs of 2018. IRENA projected a 59% investment cost reduction for Solar PV and 43% for CSP between 2015 and 2025 [79], which would imply a LCOE reduction in the order of magnitude of 40% and 30% between 2018 and 2025 for PV and CSP+TES respectively. A much more conservative approach is taken in this study, considering only a 15% overall reduction of solar PV LCOE in 2025 compared to 2018 aligned with expected LCOE of solar PV in Chile by that year estimated by Bloomberg [56] and Tractebel [39] and a 10% reduction for CSP + TES in 2025, in line with the projections by Lilliestam et al. [80], Gallardo et al [37] and Benavides et al. [36].

### Water electrolysis

Water electrolysis (low temperature) is amongst the mature technologies for hydrogen production. If coupled to renewable electricity it represents a viable pathway for zero-emission green-H<sub>2</sub> production. By applying an external voltage upon a pair of electrodes immersed in an ionic conductive electrolyte the electrochemical decomposition of water into H<sub>2</sub> and O<sub>2</sub> is obtained. The steady state specific electricity consumption for H<sub>2</sub> production depends on the electrolyser type and thermodynamic operating conditions (temperature and pressure) [6,81–83]. The system specific energy consumption parameters (including auxiliaries [84]) reported in literature for ALK and PEM electrolysers are equal to 54 kWh/kg<sub>H2</sub> and 60 kWh/kg<sub>H2</sub> (2018) and 49 kWh/kg<sub>H2</sub> and 52 kWh/kg<sub>H2</sub> (2025) for ALK and PEM respectively, as reported in Table 2 [6,8,20–22,49,50,81,82,84], which include auxiliaries. Fixed stack and auxiliary consumptions lead to a constant efficiency equal to the ratio as shown in Eq. (1).

$$\eta_{el} = \frac{LHV_{H_2}}{C_{sp,el}} \quad (1)$$

where  $C_{sp,el}$  (kWh/kg) is the system Specific Energy Consumption “SEC” (including auxiliaries) reported in Table 2 and  $LHV_{H_2}$  is the lower heating value of hydrogen, equal to 33.33 kWh/kg<sub>H2</sub>. In nominal conditions the system efficiency is equal to 61% for ALK and 55% for PEM in 2018 and 67% for ALK and 63% for PEM in 2025, in line with analysed literature [6,8,20–22,49,50,81,82,84].

From  $C_{sp,el}$  it is possible to calculate the mass flow of hydrogen  $\dot{m}_{H_2}$  (kg/h) considering the instantaneous power profile of the electrolyser  $P_{el}$  (kW) by applying Eq. (2):

$$\dot{m}_{H_2} = \frac{P_{el}}{C_{sp,el}} \quad (2)$$

The obtained H<sub>2</sub> is obtained in kg or Nm<sup>3</sup> (referred to 101.325 kPa and 0 °C) related by constant density in normal conditions equal to 0.0898 kg/Nm<sup>3</sup>. In fact, within the

<sup>1</sup> The SAM simulation has been validated by NREL with MW-scale solar tower CSP plants [69], in line respect to the Cerro Dominador plant – 110 MW<sub>e</sub> – in construction in the Atacama Desert Region in Chile [36,37,61].

**Table 2 – Electrolyser Parameters [6,8,20–22,49,50,81,82,84].**

Electrolyser performance parameters		ALK	PEM
System specific consumption (w/auxiliaries)	kWh <sub>AC</sub> /kg	54 (2018) 49 (2025)	60 (2018) 52 (2025)
Stack lifetime	Operating hours (h)	80,000	65,000
Load threshold	% P <sub>n</sub>	20%-100%	0%-100% <sup>a</sup>
Specific cost	kUS\$/kW	0.52-0.65 (2018)	0.77-1.1 (2018)
	(PV-CSP coupling)	0.50-0.45 (2025)	0.7-0.56 (2025)

<sup>a</sup> PEM electrolyzers can be overloaded for limited amount of time [6,21,49,50,83], reports the capability of reaching 160% of nominal power for 10-30 minutes, however only 100% capability has been considered since the timestep of the model is 1 hour.

considered range of temperature and pressure the gaseous H<sub>2</sub> can be considered as an ideal gas.

In order to obtain the target amount of yearly cumulative H<sub>2</sub> produced, the installed power of the solar system will differ significantly for PV or CSP + TES coupling, due to the very different capacity factor profiles of solar PV and CSP + TES plants (see Fig. 2).

The Techno-Economic parameters of the electrolyzers are reported in Table 2 [6,8,20–22,49,50,81,82,84]. Both technologies are able to produce H<sub>2</sub> at 30 bar and consume around 10 lt<sub>H<sub>2</sub>O</sub>/kg<sub>H<sub>2</sub></sub>. ALK technology is more durable, with 80,000 hours of stack lifetime respect to 65,000 hours for PEM but are limited in the load range, the system cannot sustain partial loads lower than 20% of the nominal power in idle operation mode. On the other hand, PEM electrolyzers presents a full load range capability. The dynamic response of both technologies (start-up, ramp-up, ramp-down, shut-down) have been neglected since both technologies can vary the power from 0-100% in less than one hour (timestep of the model and available data) [6,21,49,50,83]. For the same reason, the temporary overloading of the PEM technology [49,50,81,83] has not been considered, given the hourly timestep of the model.

The determination of the specific CAPEX values is not trivial. Most analysed literature adopt a cost function curve in polynomial or exponential form obtained from real data; however, due to the low development of the large-scale electrolysis sector (only few multi-MW projects have actually been deployed [4]) the fitting approach is limited to the available stack power in the market (up to the order of 1-10 MW), hence not applicable due to mismatch in scale (the export case study entails installed powers of the order of 150-450 MW). For example Felgenhauer et al. and Eypasch et al. [85,86] analyse real data of kW-scale electrolysis reaching up to a scale of a few MW-scale, for which the cost curve is much steeper (up to >9 kUS\$/kW for few kW reducing up to around 0.9 kUS\$/kW between 1-2 MW scale) and presents large scaling factor exponents (up to 0.5 in [86]). Detailed analysis of CAPEX data provided by Proost [20] shows a linear cost trend reaching around 1 kUS\$/kW at 2 MW for PEM electrolyzers. In Gotz et al. [6] a comprehensive review of specific investment costs from both literature and industry is given, resulting around 0.7-1.05 kUS\$/kW for ALK and 1.2-1.5 kUS\$/kW for PEM. However, when analysing the multi-MW scale (i.e. multi-stack modules), is not straightforward, realistic costs are difficult to estimate in lack of real market data due to the intrinsic upper limit power of 1-2 MW given by the single stack [20]. Thus it is

necessary to refer to cost projections scenarios [8,22,49,50], cost projection curves [20,83] or expert elicitations [21] which are not as accurate as data driven cost fitting. The reported specific CAPEX in major energy outlooks [8,49,50] for multi-MW scale in 2017-2018 are between 500-700 US\$/kW for ALK and around 1000 US\$/kW for PEM, with a reduction in 2025-2030 of the cost up to 400-500 US\$/kW for ALK and 650-750 US\$/kW for PEM. Such results are in line with the founding literature: a piecewise linear projection for multi-MW scale PEM is presented in Proost [20] reporting a specific CAPEX of below 500 US\$/kW for 100 MW as well as in industry references [22]; cost projections in Buttler et al. [83] and Element Energy [22] range between 400-800 US\$/kW for ALK and between 500-1300 US\$/kW for PEM in the multi-MW scale. The foreseen cost reduction for 2025 is around 20% for ALK and up to 30% for PEM, reducing the investment cost gap between the two.

Therefore, instead of reporting a cost curve (which would be unrealistic in the MW scale) the cost reduction related to the increase in scale between PV and CSP coupled systems (2-3 fold) is estimated based on Proost [20] which analyses the scale-up of existing multi-stack modules of 2 MW (ALK) and 0.7 MW (PEM) based on industrial pricing indications (ITM power, NEL); the results show that a reduction of the specific CAPEX of 20% for PEM and 10% reduction for ALK is obtained, considering a 3-fold capacity increase in the MW scale.

Ultimately, the considered range of specific CAPEX reported in Table 2 is aligned with the assumptions done by other comparable references such as Acil Allen [12] which considers 650 US\$/kW for 100 MW scale, Hydrogen Council [17] which estimates 500 kUS\$/kW in 2030 and Tractebel [39] which considers 550 US\$/kW in 2023 based on industrial indications claimed by NEL [87] reporting <500 US\$/kW in 2020 for its 400 MW alkaline electrolyser.

OPEX costs include solar electricity cost (Table 1), O&M cost - calculated as 2% of the initial CAPEX per year and stack replacement cost - equal to 45% and 30% of the initial CAPEX for ALK and PEM, respectively, once reached the stack lifetime [8,49,50]. Due to water scarcity in the Atacama Region [88], the supply of water is considered via reverse osmosis desalination of seawater to avoid hazardous impact on the regional water availability: the levelised cost of desalinated water cost is estimated at 3 US\$/m<sup>3</sup>, in line with the cost of desalinated water reported by Tractebel [39] and Campero and Harris [89] in the same area. The water cost is three times the freshwater cost in the coastal areas, which ranges between 1-2 US\$/m<sup>3</sup>

[89]. Since several studies [61,71,89] have reported that the desalinized water cost in the mainland can increase drastically (up to 10 US\$/m<sup>3</sup>) the variation such cost is considered in the sensitivity analysis (Sensitivity analysis section) assessing its impact on the LCOH. The financial cost must be considered, considering an overall WACC (Weighted Average Cost of Capital) of 5.12% which includes the effects of a 70/30 debt/equity capital structure, inflation rate and taxation on a time horizon of 20 years.

## Distribution, storage and transport

In this chapter, different supply chain distribution, storage and transport pathways are analyzed. The analysis is separated between a domestic distribution from the electrolyser plant and the long-haul transport phase by ship up to the port of arrival of Osaka, JP in different vectors. The analyzed hydrogen vectors are: LH<sub>2</sub> and liquid NH<sub>3</sub> obtained by catalysed Haber-Bosch “HB” process. The energy required for each pathway is supplied according to Table 1.

Both technologies require pre-compression of the gaseous hydrogen according to the process operating conditions or may involve a gaseous storage unit as a constraint for the conditioning process itself (HB process flexibility requirement). Also, a hybrid case (PV+CSP) is assessed via the implementation of a CGH<sub>2</sub> buffer storage which decouples the production and conditioning (liquefaction, ammonia synthesis) units.

In the direct connection cases, the H<sub>2</sub> production and conditioning plants are located onsite together with the analysed PV plants. The average distance between a solar plant in the Atacama Region and port of departure of Antofagasta is equal to 450 km. Instead, with the indirect connection scheme, since the power and H<sub>2</sub> production are decoupled [56], the electrolysis and H<sub>2</sub> conditioning plants (compression, liquefaction, NH<sub>3</sub> synthesis, see Distribution, storage and transport section) can be located in strategic locations respect to the selected distribution and transport routes. For this study the H<sub>2</sub> conditioning units are located on the coastline, an average distance of 150 km has been considered to the port of departure of Antofagasta.

The techno-economic parameters of the H<sub>2</sub> conditioning systems are reported in Table 3:

With the same approach adopted for H<sub>2</sub> production, the sizing and configuration of the liquefaction and transportation

systems was determined coupled to each electrolyser scenario (ALK and PEM), downstream the solar energy source (PV and CSP + TES). Liquefaction capacities (kg/h) were obtained from the inlet H<sub>2</sub> mass flow in function of the capacity factor.

## Compressed hydrogen

For the compression step, a multistage intercooled compressor was considered. The inlet pressure is equal to the electrolyser H<sub>2</sub> outlet pressure (30 bar). The outlet pressure depends on the H<sub>2</sub> storage form: for the liquefaction a pre-compression to 100 bar is considered whereas for the ammonia synthesis a pre-compression up to 350 bar is considered. An adiabatic and isentropic compression process is considered, characterized by Eq. (3) where  $L_{e,spec}$  is the calculated specific energy consumption of the compressor (kWh<sub>e</sub>/kg),  $\beta$  is the compression ratio,  $T_1$  is the inlet temperature equal to the ambient temperature (K),  $T_2$  is the outlet temperature (K),  $n$  number of compression stages equal to 3,  $k$  the ratio of  $c_p$  and  $c_v$ , the specific heat values (kWh/kg K) of the gas. The specific heat values ( $c_p$  and  $c_v$ ) are calculated at the average temperature  $T_m$  between  $T_1$  and  $T_2$ . The thermodynamic properties of hydrogen were obtained using CoolProp library. The mechanical and electrical efficiency terms  $\eta_m$  and  $\eta_e$  of the compressor are assumed constant and equal to 70% and 90%, respectively.

$$L_{e,spec} = \frac{c_{pH_2} \Delta T_{12}}{\eta_m \eta_e} = \frac{T_1 \left( \beta^{\frac{k-1}{k}} - 1 \right)}{\eta_m \eta_e} \quad (3)$$

After a first assumption of  $T_2$ , the equation is solved iteratively in order to update the value of  $c_p$  at the average temperature  $T_m$  between  $T_1$  and  $T_2$ . The iterative process is repeated until the variation of  $c_p$  is negligible.

The specific CAPEX considered for the compressor unit is 3.9 kUS\$/kW<sub>e</sub>, as reported by Reuß et al [9] and Ikaheimo et al. [28]; where the installed capacity is obtained in function of the hydrogen flow rate and the electrical consumption assessed via Eq. (3), according to inlet and outlet pressures. The OPEX is composed of energy cost, according to Eq. (3) and O&M, assessed at 4% of the CAPEX, annually. The specific CAPEX of the steel storage tanks for compressed hydrogen up to 350 bar is estimated equal to 500 US\$/kg [15,28], with a yearly O&M cost equal to 2% of the CAPEX. The Techno-Economic parameters are summarized in Table 3.

**Table 3 – Hydrogen conditioning systems, techno-economic parameters [15,24,25,28,51,90,91].**

System	Pressure (bar)	Specific cost	SEC	O&M (%CAPEX)	comments
Compr. unit	Up to 350 bar	3900 US\$/kW <sub>e</sub>	Eq. (3)	4%	<ul style="list-style-type: none"> <li>Multi-stage intercooled</li> <li>Adiabatic isentropic</li> <li><math>\eta_m=70\%</math>; <math>\eta_e=90\%</math>;</li> </ul>
CGH <sub>2</sub> storage	Up to 350 bar	500 US\$/kg <sub>H2</sub>	-	2%	-
Liquef. unit	82	50 kUS\$/ (kg/h)	6.4 kWh <sub>e</sub> /kg <sub>H2</sub>	4%	$p_{in}$ 30 bar
LH <sub>2</sub> storage	≈ 1 bar	90 US\$/kg <sub>H2</sub>	-	4%	Boil-off 0.1-0.2%/day
NH <sub>3</sub> synthesis unit	200-350	3500 US\$/ (kg <sub>NH3</sub> /h)	0.64 kWh <sub>e</sub> /kg <sub>NH3</sub>	2%	<ul style="list-style-type: none"> <li>3 flexibility scenarios</li> <li>Firm-up electricity 100 US\$/MWh</li> </ul>

### Liquefied hydrogen

The liquefaction step is based on the data of the IDEALHY project presented by Stolzenburg et al. [24] which propose a two-stage cooling system with flash separation of LH<sub>2</sub>, the obtained flash separation rate is equal to 95%, while the 5% unconverted vapour enters a flash gas cycle to be successively liquified. The system operated with a pre-compression at to 80 bar before the pre-cooling phase with crossflow mixed refrigerant (nitrogen, methane, ethane, propane and butane) and Nelium (75% helium, 25% neon) streams, successively the temperature of the H<sub>2</sub> flow is further reduced to 26.8 K by the cryo-coolers, the cooling is performed by two overlapping Brayton cycles with a common compression train. The capacity studied in the IDEALHY project is 50 ton<sub>H<sub>2</sub></sub>/day of liquid hydrogen, similar to the capacity considered in the present study equal to 44 ton<sub>H<sub>2</sub></sub>/day. The results of Stolzenburg et al. show that the specific energy consumption of the optimized 50 ton<sub>H<sub>2</sub></sub>/day system can reach 6.76 kWh<sub>e</sub>/kg<sub>H<sub>2</sub></sub> at full load operation. The initial pressure plays an important role in specific energy consumption value, in fact an initial pre-compressed gas at 30 bar avoids the energy consumption due to compression and lowers the full load consumption to around 6.4 kWh<sub>e</sub>/kg<sub>H<sub>2</sub></sub>. In a conservative manner, 6.4 kWh<sub>e</sub>/kg<sub>H<sub>2</sub></sub> is taken as reference specific energy consumption. The value is in line with Reuß et al [9], which consider 6.76 kWh<sub>e</sub>/kg<sub>H<sub>2</sub></sub> and with IEA [90] which reports 6.1 kWh<sub>e</sub>/kg<sub>H<sub>2</sub></sub>.

The CAPEX of the LH<sub>2</sub> plant is taken from Reuß et al [9], which presents a comprehensive set of linear CAPEX costs in function of plant capacity (ton<sub>H<sub>2</sub></sub>/day) based on project [24,91] references. The chosen value is 105 MUS\$ for a 50 ton<sub>H<sub>2</sub></sub>/day plant, equating to a specific CAPEX equal to 50 kUS\$/(kg/h). The total CAPEX is calculated according to the maximum H<sub>2</sub> flow rate for each configuration (Table 9). The CAPEX value is similar to IEA [90] which reports a specific CAPEX of 47 kUS\$/(kg/h) for large scale liquefaction plants (over 700 ton/day), showing that a substantial increase in capacity does not entail a substantial reduction of the specific CAPEX. A fixed annual cost O&M equal to 4% of CAPEX was used as reported by Stolzenburg [24] and IEA [90]. The energy cost is calculated for each case at its representative electricity cost, reported in Table 1.

### Ammonia carrier

In the ammonia (NH<sub>3</sub>) carrier case, hydrogen is stored chemically via the synthesis of ammonia, with significative advantages in terms of hydrogen mass content and stability of the carrier. In fact, liquid NH<sub>3</sub> at transport conditions – 25°C

and 10–20 bar – presents a mass density of around 680 kg/m<sup>3</sup>, the H<sub>2</sub> mass content in NH<sub>3</sub> is 18% from stoichiometry [92], resulting in an equivalent H<sub>2</sub> density of 122.4 kg/m<sup>3</sup> which is 70% higher respect to the liquid hydrogen density (which requires more extreme operating conditions presenting a boiling point of -253 °C at 1 atm), equal to 71.4 kg/m<sup>3</sup> [26]. On the contrary, the additional cost and complexity of NH<sub>3</sub> synthesis and subsequent decomposition at the port of arrival must be added to the supply chain in its entirety.

Typically NH<sub>3</sub> production plants based on the Haber-Bosch “HB” process are large plants (with capacities of the order of 1000–2000 ton<sub>NH<sub>3</sub></sub>/day) operating in steady state under standard operating conditions of 200–350 bar and 400–500 °C, over an iron-based catalyst [19,29,93,94]. The H<sub>2</sub> feedstock in such plants is typically obtained by Steam Methane Reforming “SMR” of natural gas [95]. However, several studies have investigated the possibility of flexible ammonia production coupled to renewable energy systems and electrolytic H<sub>2</sub> feedstock [19,29,92], as shown in Fig. 3. The CAPEX of the plant is affected relevantly due to the absence of the reformer (which can represent up to 50% of the total cost) and the extra storage capacity in function of the degree of flexibility of the HB process (no, standard and high flexibility cases as defined by Armijo and Philibert [25] and later described in this section). Although the process is exothermic, the HB synthesis and air separation unit components require an electrical consumption equal to 0.64 MWh<sub>e</sub>/ton<sub>NH<sub>3</sub></sub> [25,28]. Such electricity supply should be guaranteed continuously and cannot be guaranteed by direct renewable sources (due to daily and seasonal variability). The H<sub>2</sub> feed is considered at the flow rates of each H<sub>2</sub> production technology coupling scenario (Table 9) and the three different flexibility cases for the HB plant are assessed for each technology coupling scenario and its respective electricity cost (Table 1). The HB unit is operated discontinuously both for the PV cases (high flexibility required or medium/no flexibility with relevant storage) or continuously for the CSP direct connection or for the PV+buffer+CSP case (medium flexibility required or no flexibility with suitable storage). Only for the PPA 24/7 the non-flexible system can be considered without additional storage since the electricity supply is guaranteed continuously (see [Chilean solar energy market section & Input data section](#)). The output NH<sub>3</sub> is stored and transported in stable liquid form at 10–20 bar and ambient temperature (see Table 3).

Standard SMR based HB plants specific CAPEX values reported by IEA [90] are around 900 US\$/ton<sub>NH<sub>3</sub></sub>, which for the considered yearly production of around 90 kton<sub>NH<sub>3</sub></sub> per year (16 kton<sub>H<sub>2</sub></sub>/year and 18% mass content in NH<sub>3</sub>) equates to around 7800 US\$/(kg/h) for steady state operation (including the reformer). Many references report large scale electrolysis-fed NH<sub>3</sub> plants total CAPEX cost between 700–900 US\$/ton<sub>NH<sub>3</sub></sub>, which equates to around 6000–7800 US\$/(kg/h). Excluding the electrolyser – which is previously considered (see [Input data section](#)) – the specific CAPEX of only the NH<sub>3</sub> conversion section (mainly HB synthesis unit and air separation unit), is reported by Ikaheimo et al. [28] between 2730 and 4100 US\$/(kg<sub>NH<sub>3</sub></sub>/h), an intermediate value equal to 3500 US\$/(kg<sub>NH<sub>3</sub></sub>/h) was used due to the lower capacities of the considered plant (around 250 ton<sub>NH<sub>3</sub></sub>/day) respect to typical NH<sub>3</sub> production plants (1000 ton<sub>NH<sub>3</sub></sub>/day [95]). However, such specific CAPEX



Fig. 3 – NH<sub>3</sub> conversion conceptual scheme



assumptions are valid only for large scale scenarios (such as the exportation one object of study), in fact Tuna et al. [96] report that smaller scale electrolytic  $\text{NH}_3$  production plants (3–10 MW electrolysis) incur specific CAPEX costs up to 4300–5000 US\$/ $(\text{ton}_{\text{NH}_3}/\text{y})$ , which equate to 35000–45000 US\$/ $(\text{kg}_{\text{NH}_3}/\text{h})$ , one order of magnitude more expensive than the considered costs. Tremel et al. [97] present a cost curve for  $\text{NH}_3$  plants from electrolytic  $\text{H}_2$  based on comprehensive review of literature data within the capacity range of 10–500  $\text{MW}_{\text{NH}_3,\text{out}}$  with the specific CAPEX between 15000 US\$/ $(\text{kg}_{\text{NH}_3}/\text{h})$  for 10  $\text{MW}_{\text{NH}_3,\text{out}}$  and 4300 US\$/ $(\text{kg}_{\text{NH}_3}/\text{h})$  for around 500  $\text{MW}_{\text{NH}_3,\text{out}}$ , in line with the considered values. Since the synthesis unit and air separation units are fully commercially developed components industrially, the CAPEX is not expected to decrease in the future [90].

The capacity (kg) of  $\text{CGH}_2$  storage must be sized in order in function of the degree of flexibility operation of the HB plant (part load capability, number of stops and dynamic operation capability). Armijo and Philibert have defined three flexibility scenarios: the no flexibility case (steady state operation), the standard flexibility case (up to 40% downwards part load capacity in discrete steps of 100%, 80% and 60% respect to nominal conditions) and the high flexibility case (up to 80% downwards and 5% upwards part load capacity respect to nominal conditions), which can be obtained without increasing the HB specific CAPEX by tuning some adjustable parameters of the operating conditions envelope (e.g.  $\text{H}_2$  to  $\text{N}_2$  ratio and operating temperature). The no flexibility and the standard flexibility cases are considered in line with the current state of the art technology, while high flexibility case is considered feasible respect to the existing technology and promising for RES-coupled  $\text{NH}_3$  conversion plants [29]. A precise determination of the storage capacity would require a dynamic simulation of the  $\text{NH}_3$  conversion plant [6,25,30], however a preliminary estimation of required storage capacity for the three flexibility cases can be obtained based on the results of Armijo and Philibert [25], which report storage capacities of up to 6 days for the no flexibility case, between 1

and 2 days of full load operation for the standard flexibility case and under 1 day of full capacity operation for the high flexibility case. The days of storage capacity have been set conservatively to 1, 4 and 8 days of full load capacity for no flexibility, standard flexibility and high flexibility scenarios, respectively. In the case of intermittent  $\text{H}_2$  supply (from PV) and flat HB operation (from CSP), the storage capacities have been increased by 20% since the storage depends from both the  $\text{H}_2$  supply variability and the HB flexibility. The  $\text{H}_2$  storage is considered in gaseous state in compressed cylinders at 200 bar, in line with the operating conditions of the HB synthesis unit. The additional cost of pre-compression to such pressure level is included in the  $\text{NH}_3$  conversion cost according to the compressor parameters described in (Compressed hydrogen section and Table 4).

The OPEX cost of the ammonia production is dependent from the production LCOH which defines the  $\text{H}_2$  feedstock cost, the electricity supply (RES and firm-up) and the O&M, calculated as 2% of the initial CAPEX per year [28]. The additional firm-up grid electricity is calculated by difference in function of the capacity factor of the coupled RES system (PV or CSP), the cost of the firm-up grid electricity is estimated equal to 100 US\$/MWh [25].

### Distribution & transport

After the liquefaction or the ammonia synthesis process, the hydrogen (as  $\text{LH}_2$  or  $\text{NH}_3$ ) must be transferred to the port of departure (Antofagasta, CL) then shipped to the port of arrival (Osaka, JP). The port management infrastructure (storage tanks and loading/unloading operations) must be sized according to the shipping frequency.

This domestic distribution phase is considered by mean of dedicated trucks. IEA [90] presents a cost function for domestic transport in function of distance for each  $\text{H}_2$  vector, considering around 0.12–0.13 US\$/ $(\text{kg}_{\text{H}_2} \cdot 100\text{km})$  for  $\text{LH}_2$  and  $\text{NH}_3$  (due to their comparable mass density), and around 0.6 US\$/ $(\text{kg}_{\text{H}_2} \cdot 100\text{km})$  for  $\text{CGH}_2$  do to its reduced mass density

**Table 4 – Ship characteristics 2018 vs. 2025 [51,90,98–102].**

	$\text{LH}_2$		$\text{NH}_3$	
	2018	2025	2018	2025
Distribution US\$/ $(\text{kg} \cdot 100\text{km})$	0.13	0.13	0.12	0.12
<b>Ship characteristics</b>				
Capacity ( $\text{m}^3$ )	2,500	160,000	2,500	53,000
CAPEX (MUS\$/ship)	21	412	21	85
O&M ships (% $\text{CAPEX}/\text{year}$ )	4%	4%	4%	4%
Distance (km)	17,500			
Speed (knots)	13	16	13	16
Round trip time (days)	60	51	60	51
Specific fuel consumption (MJ/km)	3090	4751/1490 <sup>a</sup>	3090	2500
Boil-off losses (%/day)	0.2%/day	0.2%/day	-	-
<b>Export/Import Port management infrastructure</b>				
Port storage CAPEX (US\$/ $\text{kg}_{\text{H}_2}$ )	90/90	90/90	9.5/9.5	9.5/9.5
O&M storage (% $\text{CAPEX}/\text{year}$ )	4%/4%	4%/4%	4%/4%	4%/4%
Charge/discharge pumps flow rate ( $\text{m}^3/\text{h}$ )	60/60	1000/1000	60/60	1000/1000
Loading operations (days)	2/2	8/8	2/2	4/4
Boil-off losses (%/day)	0.1%/0.1%	0.1%/0.1%	-/-	-/-
Specific energy consumption (kWh/ $\text{kg}_{\text{H}_2}$ )	0.61/0.2	0.61/0.2	0.005/0.02	0.005/0.02
<sup>a</sup> $\text{H}_2$ boil-off propulsion ship				

**Table 5 – NH<sub>3</sub> reconversion parameters [90,104].**

Parameter	Unit	Value
Specific cost	MUS\$/(ton <sub>NH3</sub> /y)	0.31
O&M	%CAPEX/year	4%
Heat requirement	kWh <sub>th</sub> /kg <sub>H2</sub>	9.7
Heat cost	US\$/MBTU	9
Electricity requirement	kWh <sub>e</sub> /kg <sub>H2</sub>	1.5
Electricity cost	US\$/MWh <sub>e</sub>	160
H <sub>2</sub> recovery rate	%	99%
PSA recovery rate	%	85%

[26]. The domestic distribution depends on the distance between the H<sub>2</sub> conditioning plants and the port of departure. Domestic distribution via gaseous H<sub>2</sub> is not considered due to the increased cost of truck distribution.

The sea transport phase is divided between the actual travel cost and the port management schemes. Both aspects greatly depend on the ship and the H<sub>2</sub> carrier characteristics. The techno-economic parameters for the transport phase are reported in Table 4. As previously described, the H<sub>2</sub> amount to be delivered at the port of arrival is set to 15 kton<sub>H2</sub>/year, however the actual transported H<sub>2</sub> amount is increased according to the carrier losses.

The 2018 ships derive from adaptation of currently existing small scale (15,000 m<sup>3</sup>) LNG ships [98] or prototype ships under development by KHI [51], while the ships foreseen for 2030 are specifically developed for LH<sub>2</sub> or NH<sub>3</sub> carrier transport as reported by IEA and KHI [51,90]. The CAPEX of the NH<sub>3</sub> ships is by far cheaper than the LH<sub>2</sub> technology (around 9 US\$/kg<sub>H2</sub> respect to 30–120 US\$/kg<sub>H2</sub> due to the carrier characteristics, operating conditions and stability which deeply affects the storage cost [92]). The H<sub>2</sub> amount carried by each ship is also different according to the selected carrier: for 2018 at equal ship capacity (m<sup>3</sup>) the H<sub>2</sub> stored in the NH<sub>3</sub> carrier is 1.7 times the one stored in the LH<sub>2</sub>; for 2025 the differences in ship capacity entail that a LH<sub>2</sub> ship transports more H<sub>2</sub> (11 kton<sub>H2</sub>) respect to the NH<sub>3</sub> ship (53,000 m<sup>3</sup>, containing around 6.5 kton<sub>H2</sub>). The specific fuel consumptions for the diesel propulsion ships were calculated by Bialystocki et al. [99] or indicated by IEA [90] and KHI [51]. The 2025 LH<sub>2</sub> ship presents an optimized propulsion system partially run on the boil-off gas, rated at 0.2%/day of the total carried H<sub>2</sub> amount, reducing the fuel consumption up to 70% [90]. The cost for IFO 380 was assumed 400 US\$/ton [100], associated with a emission factor equal to 322 kg<sub>CO2</sub>/ton [103], the total fuel consumption is calculated in relation to the travel time and the LHV of the fuel which is around 12 kWh/kg. Considering the cruise speed of 13–16 knots the travel time (round-trip) is equal to 51–60 days.

In terms of port management infrastructure, the required time for loading/unloading the ship is calculated based on the charge/discharge pumps flow rate. Considering 60 m<sup>3</sup>/h for pumps usually used for small-scale loading bays/bunkering ships for 2018 and 1000 m<sup>3</sup>/h for large-scale LNG cargo feeding systems for 2030 [101,102] a total duration of the loading/unloading phase is estimated at 2 days for 2018 and 8 days for 2030 for LH<sub>2</sub> (net of the boil-off losses), which is in line with other references [98,101,102]. For the loading of liquid ammonia, the port infrastructure is simplified thanks to the increased mass density and stability of the chemical carrier.

The duration of the loading/unloading phase, considering the same flow rates is 2 days for 2018 and 4 days for 2025, in function of the ship capacity (m<sup>3</sup>). Considering the daily production of 44 ton<sub>H2</sub>/day, the storage sizing (ton) in the port is determined equal to the difference between the ship capacity and the direct production in the required time for loading [90].

The boil-off losses for LH<sub>2</sub> (Table 5) are calculated during the whole round-trip time, the losses amount to 0.1%/day during storage in the import/export terminal and 0.2%/day during half of the sea transport travel time [51,90]. Considering the travel and storage time and storage reported in Table 4, the boil-off losses amount to around 1 kton<sub>H2</sub>/year, in all cases, which is around 6% of the total demand.

Transport via ammonia carrier does not incur with boil off losses thanks to the stability of the carrier at transport operating conditions (25 °C, 20 bar), however reconversion losses must be assessed (Table 5) in relation to the recovery rates of the inverse HB decomposition (H<sub>2</sub> recovery rate 99%) and the PSA separation (H<sub>2</sub> recovery rate 85%), shown in Table 5. Considering the total losses (total losses around 16%) in order to cover the demand of 15 kton<sub>H2</sub>/year the total H<sub>2</sub> produced should be around 17.85 kton<sub>H2</sub>/year, with an increase of around 2.85 kton<sub>H2</sub>/year (total H<sub>2</sub> recovery rate around 84%).

Furthermore, to obtain a comparable cost (H<sub>2</sub> delivered in the port of arrival) the ammonia decomposition at the port of arrival should be assessed, extracting H<sub>2</sub> from the NH<sub>3</sub> carrier. The reconversion process is endothermal and requires both process heat (9.7 kWh<sub>th</sub>/kg<sub>H2</sub>) and electrical power for the PSA system (1.5 kWh<sub>e</sub>/kg<sub>H2</sub>). The cost of industrial heat is estimated at 9 US\$/MBTU based on the natural gas cost trend and electricity cost for industrial users in Japan is reported equal to 160 US\$/MWh<sub>e</sub> [104]. Techno economic parameters of ammonia reconversion are reported in Table 5 [90].

The reconversion losses (16%) are nearly three times the boil off losses (6%). However, the disadvantage of increased losses for reconversion is balanced by the advantageous increased mass density in the ammonia carrier (70% more H<sub>2</sub> content in mass) and its stability which strongly reduce the transport and storage cost [92].

If the ammonia is used in Japan directly (as chemical in industrial processes, as feedstock for fuel cells, co-fired coal/ammonia plants or NH<sub>3</sub>-fed gas turbines [46]) the reconversion cost could potentially be avoided.

## Results and discussion

The Techno-Economic Analysis is performed for all the analysed H<sub>2</sub> supply chain pathways, calculating the LCOH throughout the various steps of the supply chain.

### Solar hydrogen production - results

The specific installed electrolysis capacity (MW<sub>e</sub>) is calculated per unit of demand (1 kton<sub>H2</sub>/year), the results are reported in Table 6:

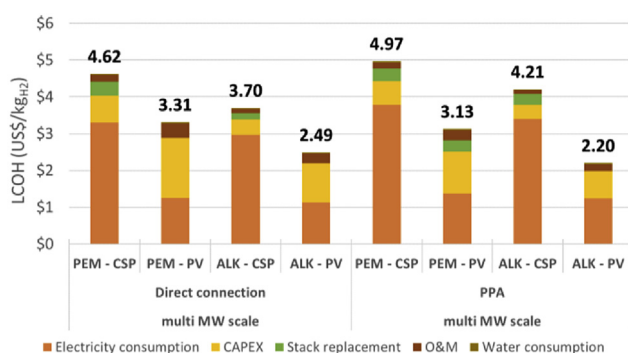
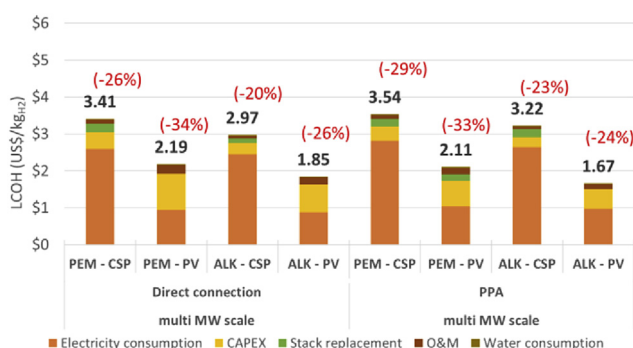
H<sub>2</sub> production from PV coupled systems (direct connection) entail a larger installed electrolyser capacity – 22.4–25.0 MW<sub>e</sub>/(kton<sub>H2</sub>/year) (2018) and 20.6–21.6 MW<sub>e</sub>/(kton<sub>H2</sub>/year) (2025) – due to the low capacity factor of PV (approx. 32%). In case of

**Table 6 – Electrolyser specific capacity requirements.**

Specific capacity 1 kton <sub>H2</sub> /year		ALK+PV direct	ALK+CSP direct	PEM+PV direct	PEM+CSP direct
Installed power MW <sub>el</sub> /(kton <sub>H2</sub> /year)	2018	22.4	8.0	25.0	9.0
	2025	20.6	7.4	21.6	7.7
		ALK+PV	ALK+CSP	PEM+PV	PEM+CSP
		PPA	PPA	PPA	PPA
		2018	7.2	17.5	8.0
		2025	6.6	15.1	6.9

**Table 7 – Electrolyser capacity requirements.**

16 kton <sub>H2</sub> /year		ALK+PV direct	ALK+CSP direct	PEM+PV direct	PEM+CSP direct
5% METI demand + boil-off losses					
Installed power (MW <sub>el</sub> )	2018	358.7	128.7	400.2	143.6
	2025	329.8	118.4	345.2	123.9
		ALK+PV	ALK+CSP	PEM+PV	PEM+CSP
		PPA	PPA	PPA	PPA
		2018	115.1	280.1	128.4
		2025	105.8	241.7	110.8

**Fig. 4 – LCOH breakdown from solar technologies (2018)****Fig. 5 – LCOH breakdown from solar technologies (2025) and reduction (%) respect to 2018**

supply via PPA solar hours (see [Input data section](#)) the installed electrolyser power is lower – 15.7–17.5 MW<sub>el</sub>/(kton<sub>H2</sub>/year) (ALK-PEM 2018) and 14.4–15.1 MW<sub>el</sub>/(kton<sub>H2</sub>/year) (ALK-PEM 2025), due to the constant supply at nominal power between 08–18h. Cumulative H<sub>2</sub> production under PV supply is discontinuous due to the intermittency of the solar resource. CSP supply, on the other hand, entails smaller size electrolyzers, the direct connected case results in 8.0–9.0 MW<sub>el</sub>/

(kton<sub>H2</sub>/year) (ALK-PEM 2018) and 7.4–7.7 MW<sub>el</sub>/(kton<sub>H2</sub>/year) (ALK-PEM 2025) thanks to higher capacity factors (above 85%) thanks to the TES. In the 24/7 PPA case from CSP, the electrolyser capacity is lowest – 7.2–8.0 MW<sub>el</sub>/(kton<sub>H2</sub>/year) (ALK-PEM 2018) and 6.6–6.9 MW<sub>el</sub>/(kton<sub>H2</sub>/year) (ALK-PEM 2025) – with 24/7 flat operation. The H<sub>2</sub> cumulative production is linear since the production is constant. PEM electrolyser capacity sizing is higher than ALK by around 11% in 2018 and around 5% in 2025, due to the lower efficiency in steady state. The power ratings of PV coupled electrolysis results 2–3 times higher than CSP + TES coupled ones in 2018, reduced to around 1.5–2 times higher in 2025 due to the improvements in the specific energy consumptions. The PPA supplied schemes are lower than the direct coupling schemes by around 30% for PV case and by 11% for the CSP case, due to the difference of the capacity factors.

Considering the total H<sub>2</sub> demand set by METI targets (300 kton<sub>H2</sub>/year) would result in a total electrolyser rated capacity of 6.2–7.5 GW if directly coupled to PV (4.3–5.3 GW if coupled indirectly via PPA) and 2.2–2.7 GW if directly coupled to CSP+TES (2.0–2.4 GW if coupled indirectly via PPA), which is unrealistically high. Considering that in the end of 2018 the installed capacity of solar PV in the Atacama Desert is 2.14 GW [34–37], if hypothetically all the plants currently installed were dedicated only to H<sub>2</sub> production about 30–40% of the Japanese market share would be covered. A market share considered feasible of in terms of actual installed capacity in the region is around 5% of the total demand [12], equal to 15 kton<sub>H2</sub>/year. The demand was increased for all scenarios by 1 kton<sub>H2</sub>/year in order to compensate the boil-off losses (see [Distribution, storage and transport section](#) for details) [51,90]. The electrolyser installed capacities required to cover a demand of 16 kton<sub>H2</sub>/year are reported in [Table 7](#).

The same considerations done for [Table 7](#) are valid, where the power range of the electrolyzers is between 330–360 MW for direct coupled PV systems and between 120–145 MW for direct coupled CSP systems, whereas between 230–280 MW for direct coupled PV systems and between 105–130 MW for direct coupled CSP systems. The LCOH is calculated for each system

coupling scenario, the breakdown of the total levelised cost is reported in Fig. 4 (2018) and Fig. 5 (2025).

The results show that, for all the scenarios, PV coupled systems are more cost-competitive than CSP + TES scenarios although the installed capacity (for an equal  $H_2$  demand) is greater due to the reduced capacity factor of PV systems (operating daily in solar hours) respect to CSP which operate with a 24/7 profile with the TES. This is thanks to the very low cost of electricity (20–25 US\$/MWh), which represents, for all cases considered, the most relevant contribution of the LCOH breakdown in production phase.

ALK + PV-PPA supply is the most cost competitive option with 2.20 US\$/kg for and 1.67 US\$/kg for 2025. The LCOH cost composition in 2018 is given mainly by electricity cost (56.4%) and CAPEX (33.9%). The remaining contribution is given by O&M (8.4%), water consumption is negligible (1.4%). Stack replacement is not required since an average PV capacity factor equal to 41% results in 3650 h/year annual operating hours, which do not sum up to 80,000 h in 20 years. The 2025 LCOH breakdown shows a relevant contraction of the CAPEX contribution (-51%) respect to electricity cost (-14%), due to the already very low cost of electricity. The PV direct connection schemes, albeit presenting a lower cost of electricity, present an over-cost between 5–15% respect to the PPA option.

The most expensive LCOH at the output of the electrolyser is given by the PPA PEM + CSP configuration, resulting a LCOH equal to 4.97 US\$/kg in 2018. This case comprises both expensive electricity cost (63 US\$/MWh from the CSP-PPA supply) and the disadvantages of PEM (lower efficiency and increased specific CAPEX). The LCOH breakdown shows that the electricity cost percentage contribution is much higher (76.1%) and the CAPEX contribution is lower (13.1%) due to the lower installed power of the electrolyser. The stack replacement cost is relevant (7.0–7.2%) since 24/7 operation entails 2 stack replacements throughout the 20 years of operation. The O&M contribution (3.2%) results swamped by the other costs and water cost contribution (0.6%) remains negligible. The CSP coupling presents an opposite trend between directly connected and PPA based schemes: direct connection results cheaper due to the high PPA price respect to the LCOE and the small increase in capacity factor.

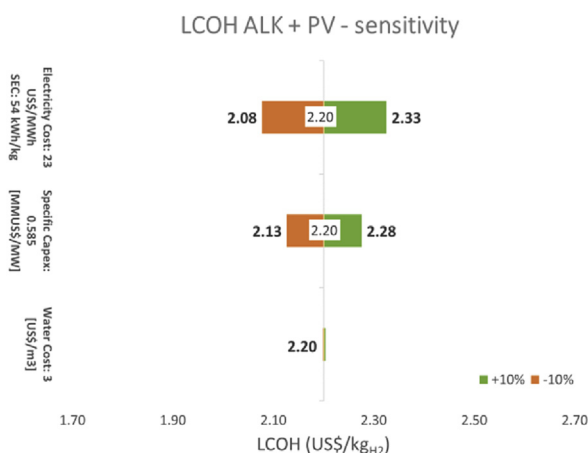


Fig. 6 – Sensitivity analysis – ALK + PV-PPA (2018)

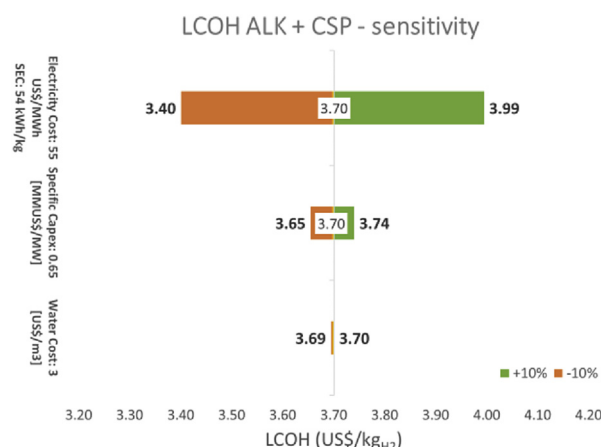


Fig. 7 – Sensitivity analysis – ALK + CSP-direct (2018)

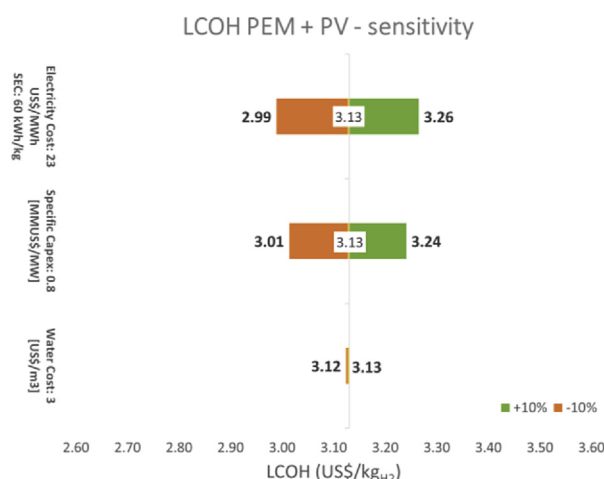


Fig. 8 – Sensitivity analysis – PEM + PV-PPA (2018)

The average reduction of the LCOH in 2025 is between 20–35% respect to 2018. A stronger reduction is expected for PEM (up to 34%) respect to ALK (up to 26%). This is due to the reduction of CAPEX and the increase of the efficiency, which is

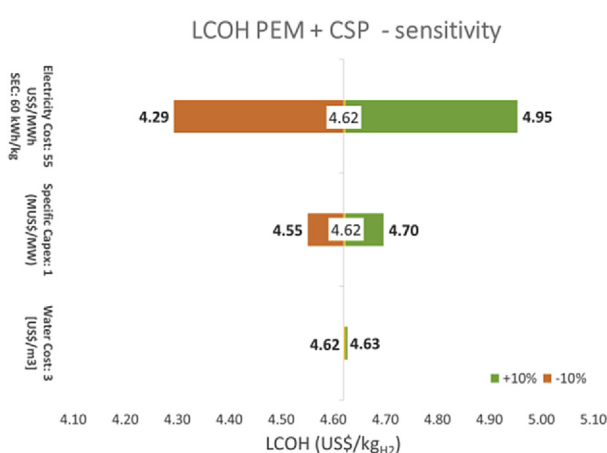


Fig. 9 – Sensitivity analysis – PEM + CSP-direct (2018)



**Table 8 – Sensitivity analysis results.**

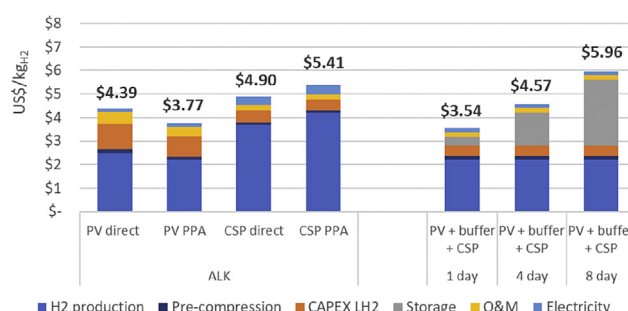
LCOH variation (%) respect to $\pm 10\%$ variation of Techno-Economic parameter		ALK+PV PPA	ALK+CSP direct	PEM+PV PPA	PEM+CSP direct
2018	SEC/Electricity cost	$\pm 5.64\%$	$\pm 8.03\%$	$\pm 4.41\%$	$\pm 7.14\%$
	Specific CAPEX	$\pm 3.39\%$	$\pm 1.15\%$	$\pm 3.63\%$	$\pm 1.57\%$
	Water cost	$\pm 0.14\%$	$\pm 0.08\%$	$\pm 0.10\%$	$\pm 0.06\%$
2025	SEC/Electricity cost	$\pm 4.71\%$	$\pm 8.24\%$	$\pm 4.94\%$	$\pm 7.62\%$
	Specific CAPEX	$\pm 3.16\%$	$\pm 1.01\%$	$\pm 3.25\%$	$\pm 1.29\%$
	Water cost	$\pm 0.18\%$	$\pm 0.10\%$	$\pm 0.14\%$	$\pm 0.09\%$

more optimistic for PEM technology. The PV coupled scenarios foresee a greater reduction (in average 29%) respect to the CSP coupled ones (in average 24%), since the oversizing of the electrolyzers are more affected by specific CAPEX reduction.

The obtained LCOH is comparable with the H<sub>2</sub> production results in the Chilean environment: Tractebel [39] calculates a LCOH equal to 1.80–3.0 US\$/kg<sub>H2</sub> in 2023, IRENA [49] calculates for H<sub>2</sub> production in Chile from hybrid PV and wind fed electrolysis an LCOH between 4–5 US\$/kg<sub>H2</sub> in 2017 with projections up to 2.5–4 US\$/kg<sub>H2</sub> in 2030. IEA [8] calculates a LCOH from renewable driven electrolysis between 1.5–3 US\$/kg<sub>H2</sub> and a potential LCOH of below 1.6 US\$/kg<sub>H2</sub> for hybrid PV + wind configurations in the long term in Chile. The Hydrogen Council [17] reports a lookup table for LCOH in function of specific CAPEX, electricity price and load factor: 2–3 US\$/kg is estimated for 20–30 US\$/MWh and load factor 30% (comparable to the PV case in Chile), while above 4–5 US\$/kg is estimated for 50–60 US\$/MWh and higher load factors (comparable to the CSP case in Chile). The Chilean solar H<sub>2</sub> results advantageous respect to other scenarios, hydrogen from offshore wind power from the Netherlands costs 2.2–2.9 US\$/kg<sub>H2</sub> in 2025, from off-peak electricity in USA 2.3 US\$/kg<sub>H2</sub> in the same period [11]. IRENA [49] reports more costly LCOH equal to 5.67–7.01 US\$/kg<sub>H2</sub> in EU in 2015.

### Sensitivity analysis

A sensitivity analysis is performed in order to quantitatively assess the impact of the parametric variation of key selected parameters upon the H<sub>2</sub> production scenarios, the PPA-based cases were considered for 2018 and the direct coupling cases were considered for CSP, since they achieve the lowest LCOH between the two supply options (direct or PPA) for that technology coupling. The selected parameters are specific CAPEX (MUS\$/MW), specific consumption (kWh/kg) or electricity cost (US\$/MWh) which both affect the electricity supply in the same way and water cost (US\$/m<sup>3</sup>). Other parameters which

**Fig. 10 – LCOH after the liquefaction step (2018)**

affect the final LCOH are O&M cost (%) which is. The SEC is equivalent to the system efficiency and the specific CAPEX indirectly includes the O&M costs, which are directly calculated from the CAPEX. The parameters were varied in a range of  $\pm 10\%$  respect to their base case values and the LCOH is recalculated. The LCOH results for 2018 in all four coupling cases (PPA), are reported in Figs. 6–9:

The sensitivity analysis results confirm that the electricity supply (which is accounted for in both the SEC and electricity cost parameters) is always the most relevant contribution – with an impact around  $\pm 7\text{--}8\%$  on the LCOH – for the CSP cases where the electricity cost is higher (55 US\$/MWh respect to 23 US\$/MWh in 2018). For CSP coupled systems specific CAPEX presents a very low impact – around  $\pm 1\text{--}1.5\%$  due to the low installed capacity. On the other hand, the PV coupled cases, are affected more relevantly by the specific CAPEX – around  $\pm 3.5\%$  – due to the oversized systems; for PEM coupling its impact is comparable with the one of electricity supply parameters (SEC/electricity cost). The impact of water cost is always below 1%, resulting negligible.

A  $\pm 10\%$  variation of the four selected techno-economic parameters are reported in Table 8 for 2018 and 2025, graphical results for 2025 are omitted for brevity.

**Table 9 – H<sub>2</sub> conditioning systems capacity requirements.**

		ALK+PV direct	ALK+CSP direct	PEM+PV direct	PEM+CSP direct
Maximum flow rate (kg/h)	2018	6642.6	2383.3	6670.0	2393.3
		6730.6	2416.3	6638.5	2382.7
	2025	6642.6	2383.3	6670.0	2393.3
		6730.6	2416.3	6638.5	2382.7
	2018	4657.4	2131.5	4668.3	2140.0
		4708.2	2159.2	4648.1	2130.8

### Distribution, storage and transport – results

With a cascading approach, the produced  $H_2$  is fed into each distribution, storage and transport pathway according to the maximum hydrogen hourly flow rates reported in Table 9, which are critical parameters determining the sizing of the distribution, storage and transport components. The average daily production for all systems is around 44 ton $H_2$ /day for  $LH_2$  and 46 ton $H_2$ /day for  $NH_3$  pathways, according to the losses (see Distribution, storage and transport section). The maximum flow rates follow the trends previously discussed for the electrolysis installed power (Tables 6 and 7).

In the following subsections, the results of each section of the supply chain is analysed in detail. Since the PEM solutions are always less cost-competitive respect to their ALK counterparts only the ALK coupled systems are analysed for the subsequent distribution, storage and transport phases.

### Compressed hydrogen – results

Compressed hydrogen is used either to reach the operating conditions of the liquefaction plant (80 bar) or the ammonia synthesis plant (up to 350 bar). Otherwise a  $CGH_2$  buffer is implemented in both the liquefaction and the ammonia synthesis case in order to decouple the  $H_2$  production and conditioning. In this way the  $H_2$  conditioning plant, which are typically best operated in steady state can be operated with a flat profile although the  $H_2$  production is intermittent.

The energy consumption for compression – calculated by Eq. (3) – from 30 to 80 bar is below 1 kWh/kg, while the consumption for compression up to 200–350 bar is within 1–2 kWh/kg. In both cases the energy consumption, as well as the CAPEX contribution of the compressor is one order of magnitude less than the energy requirement for production (see Table 2) and in any case lower than the energy requirement of other conditioning units. The CAPEX of the  $CGH_2$  storage units can become relevant for cases which require many days of storage (see Liquefied hydrogen – results section, Ammonia carrier – results section).

### Liquefied hydrogen – results

In Fig. 10, the LCOH downstream the liquefaction step is reported for 2018. Liquefaction plant capacities between 44–140 ton/day are assessed. The liquefaction LCOH contribution ranges between 1.10 US\$/kg for both CSP direct and CSP PPA, and 1.43–1.73 US\$/kg, for PV-PPA and PV direct respectively. The hybrid solution – production fed by PV-PPA and

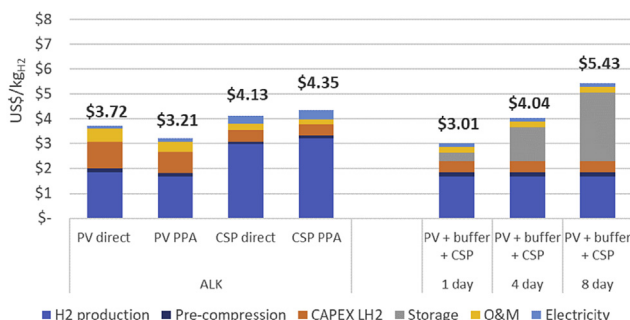


Fig. 11 – LCOH after the liquefaction step (2025)

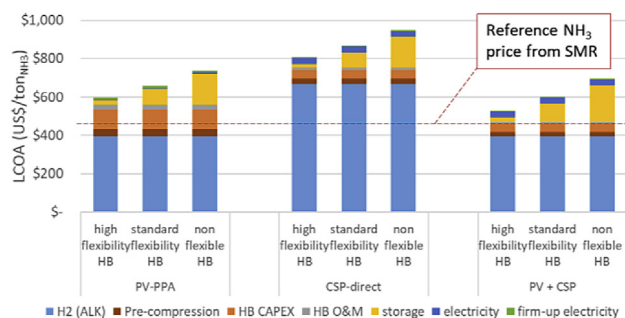


Fig. 12 – LCOA (2018) vs reference  $NH_3$  price from SMR

liquefaction fed by CSP-PPA with 1-day buffer – contribution is equal to 1.18 US\$/kg with 1-day  $CGH_2$  storage buffer. A 1-day buffer is sufficient for the PV-PPA cases since the PPA ensures the constant energy supply between 8–18h throughout the year, however an increased storage is necessary to couple direct energy supply, due to the increased variability (daily and seasonal).

The liquefaction CAPEX and O&M contributions for the PV coupled cases (due to increased flow rate) amounts up to 1.3–1.5 US\$/kg $H_2$  and is nearly double respect to the CSP coupled systems. The CSP scenarios show larger cost of electricity for liquefaction, which amounts to around 0.35 US\$/kg $H_2$ , respect to around 0.2 US\$/kg $H_2$  for PV systems. Among the simulated scenarios for  $LH_2$ , the lowest LCOH is obtained for the hybrid case with a 1-day buffer, equal to 3.54 US\$/kg $H_2$ . Despite the additional cost for the storage unit (0.35 US\$/kg $H_2$  – not negligible), the system coupling is able to achieve low CAPEX based on 24/7 operation and low electricity cost due to PV-PPA pricing (23 US\$/MWh). For larger capacity storage units (4- or 8-day capacity) the hybrid solution LCOH is strongly increased by the storage cost (1.39–2.78 US\$/kg $H_2$ ) which compromises the competitiveness respect to the PV cases. Pre-compression 80 bar does not entail a significant cost (between 0.1–0.2 US\$/kg $H_2$ ).

The results show how the liquefaction process is a CAPEX intensive operation and is more affected by a decrease in cost (due to increased capacity factor) than by a decrease in the cost of electricity. For this reason, operating with a flat profile, as guaranteed by the CSP case, ensures lower costs. In Fig. 11 the  $LH_2$  levelised costs are reported for each supply chain pathway. The results follow a similar trend discussed for 2018, with an overall cost reduction between 10–15%.

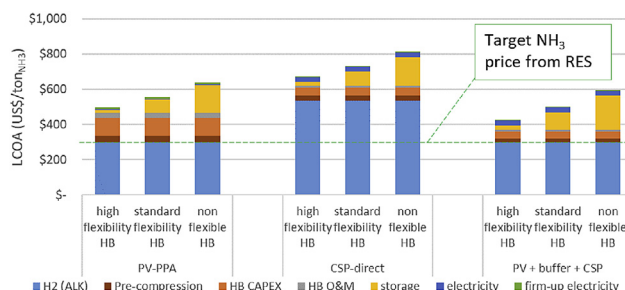


Fig. 13 – LCOA (2025) vs target  $NH_3$  price from RES

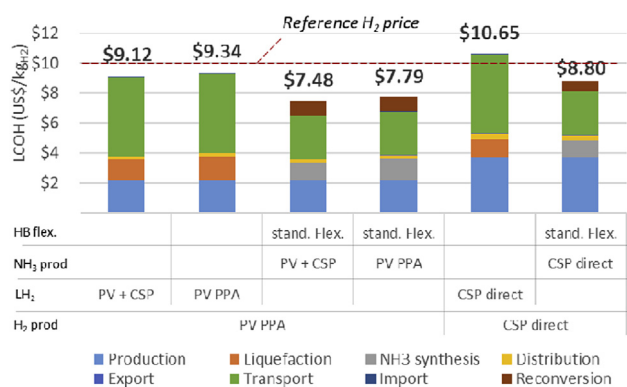


Fig. 14 – LCOH for exportation case study at Osaka, Japan (2018)

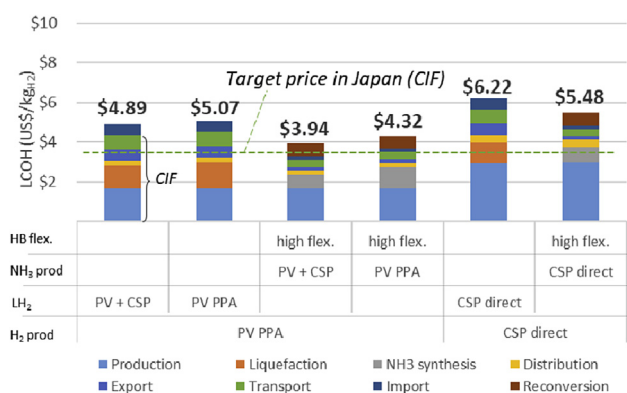


Fig. 15 – LCOH for exportation case study at Osaka, Japan (2025-2030)

The liquefaction costs contributions are in line with the results of Cardella et al [27] which report a cost range between 1.38–1.72 €/kgH<sub>2</sub> which consider electricity prices of 50–100 €/MWh respectively.

#### Ammonia carrier – results

In Fig. 12 the Levelised Cost Of Ammonia “LCOA” is calculated (only the best cases PV-PPA and CSP-direct have been considered for brevity, other than the hybrid solution PV+buffer+CSP). The NH<sub>3</sub> synthesis capacity is around 240 ton<sub>NH3</sub>/day for the CSP coupled systems and around 600 ton<sub>NH3</sub>/day for the PV coupled systems.

Similarly to what discussed for the liquefaction, the ammonia production is a CAPEX intensive process, favouring the CSP supply schemes. The synthesis of ammonia LCOH contribution ranges between 0.73 US\$/kgH<sub>2</sub> for flat energy supply schemes (CSP and hybrid PV+buffer+CSP scheme) and up to 1.89 US\$/kgH<sub>2</sub> from PV. Lower electricity cost PV supply schemes are not favoured due both CAPEX intensity and constant electricity required by the plant, which supplied by costly firm-up electricity (around 60% of the total energy supply of 56 GWh/year, at 100 US\$/MWh) for large part of the day. The most cost-competitive pathway is the hybrid one, obtaining a LCOA of 528 US\$/ton<sub>NH3</sub> which is fairly close to the reference value for SMR fed HB plants of 450 US\$/ton<sub>NH3</sub> [25], strongly dependent from the variable cost of natural gas.

However, fully flexible HB plants are not market-standard today, which could lead to unrealistically low LCOA. The results show that cost of storage is not negligible and increases rapidly with the required days of storage, reducing the degree of flexibility of the HB unit, especially for the hybrid case which presents an oversized storage to account for both the power variability and the HB flexibility [25].

The LCOA results for 2025 are reported in Fig. 13, the results follow the same trend discussed for Fig. 12, with an average reduction of around 15%, mainly due to the cost reduction of the inlet H<sub>2</sub>. The target cost for RES-driven ammonia production is set by IEA [8] at 300 US\$/ton<sub>NH3</sub>.

The LCOA results obtained for 2025 are comparable with the results obtained by [25,28,105], which report LCOA values in the range of 500–700 US\$/ton<sub>NH3</sub> in various renewable powered ammonia synthesis scenarios, including flexible electricity supply configurations.

#### Distribution & transport – results

In the following Figs. 14 and 15 the results for the final LCOH for 2018 and 2025 are reported at the port of arrival of Osaka, JP. Only the most competitive results for PV and CSP for each carrier are shown, including the hybrid case PV+CGH<sub>2</sub> buffer+CSP which achieve the most cost-competitive scenario for both carriers (LH<sub>2</sub> and NH<sub>3</sub>).

The LCOH of the NH<sub>3</sub> carrier is 7.478–7.79 US\$/kgH<sub>2</sub>, which is the lowest LCOH obtained in 2018. The cost of NH<sub>3</sub> synthesis (1.13–1.45 US\$/kgH<sub>2</sub>) and reconversion (around 1 US\$/kgH<sub>2</sub>) is balanced with a reduced distribution, import/export and travel cost (only 3.14 US\$/kgH<sub>2</sub> in total) thanks to the chemical carrier characteristics. The standard flexibility HB unit is considered (in line with the current state of the art of the technology), which includes a 4-day CGH<sub>2</sub> buffer (around 0.4 US\$/kgH<sub>2</sub>) both to smoothen the supply to the synthesis plant and in relation with the HB flexibility degree. Non-flexible HB units would require a further increase of the storage capacity (up to 8-day at full load capacity), increasing the cost by around 0.4–0.5 US\$/kgH<sub>2</sub>.

The LH<sub>2</sub> scenarios present a LCOH range between 9–10 US\$/kgH<sub>2</sub>. The liquefaction process accounts for around 1.5 US\$/kgH<sub>2</sub> in total, which is 30–40% lower than the sum of NH<sub>3</sub> synthesis and decomposition cost. However, the LCOH in Japan is strongly affected (5 US\$/kgH<sub>2</sub>) by the transport contribution.

Both cases deriving from CSP driven H<sub>2</sub> production are less cost competitive respect to the PV ones. The final LCOH for the CSP coupled LH<sub>2</sub> pathway (best case) is slightly above 10 US\$/kgH<sub>2</sub>, while for the NH<sub>3</sub> pathway the final cost amounts to 8.62 US\$/kgH<sub>2</sub>. The domestic distribution cost is increased (0.38 US\$/kgH<sub>2</sub> respect to 0.19 US\$/kgH<sub>2</sub> due to the location of the H<sub>2</sub> production and conditioning plants).

The transport cost in 2018 is the dominant cost of the LCOH breakdown, accounting between 50–60% and 40% for the LH<sub>2</sub> and NH<sub>3</sub> cases, respectively. Due to the smaller capacity of the ships (2,500 m<sup>3</sup>) the LH<sub>2</sub> carrier requires 15 ships 94 shipments per year and consequently a large amount of fuel consumption (1,260 ton/shipment, equating to 405.7 ton<sub>CO2</sub>/shipment). Instead, for the NH<sub>3</sub> carrier case, the transport cost is strongly reduced related to the increased H<sub>2</sub> content in mass laden in the same ship capacity (m<sup>3</sup>). The shipping requirement is



lowered to 9 ships performing 52 shipments per year, which consequently entails a relevant reduction in CAPEX and fuel cost (the total LCOH contribution for ship CAPEX, O&M and fuel is reduced from 5.24 US\$/kg<sub>H2</sub> to 2.91 US\$/kg<sub>H2</sub>).

Due to the small ship capacity in 2018, the import/export costs are low (only around 80 ton<sub>H2</sub> storage units at the ports are required) since nearly half of the ship can be loaded/unloaded with the direct daily hydrogen production (44 ton<sub>H2</sub>/day) in the considered loading/unloading time (2 days).

All analyzed PV cases are cost-competitive respect to the 2018 reference hydrogen retail price for 2018, equal to 10 US\$/kg<sub>H2</sub>. For CSP only the NH<sub>3</sub> pathway is cost-competitive respect to the reference price, showing that it is more advantageous to use the constant energy supply from CSP schemes complementarily to PV for the H<sub>2</sub> conditioning systems rather than developing a H<sub>2</sub> supply chain directly based on CSP.

Also in 2025 the NH<sub>3</sub> carrier supplied with PV case is the most cost-competitive pathway, resulting in a LCOH as low as 3.94–4.32 US\$/kg<sub>H2</sub>. The advanced flexibility case has been considered according to the increase of RES-driven flexible ammonia production [19,29,92]. The reconversion cost accounts for around 0.66 US\$/kg<sub>H2</sub> in line with IEA [90]. The LH<sub>2</sub> pathways achieve a final LCOH of between 4.89–5.07 US\$/kg<sub>H2</sub>. Pathways from CSP driven H<sub>2</sub> production reach a LCOH of 5.48 US\$/kg<sub>H2</sub> and 6.22 US\$/kg<sub>H2</sub> for NH<sub>3</sub> and LH<sub>2</sub> carrier, respectively.

The overall reduction of the LCOH respect to 2018 is around 30–40%. The H<sub>2</sub> production shows a relevant cost reduction of 20–25% as discussed in [Solar hydrogen production - results section](#) while LH<sub>2</sub> and NH<sub>3</sub> production cost show mild reductions (within 10–15%) as discussed in the respective [Liquified hydrogen – results section](#), [Ammonia carrier – results section](#). The greatest cost contraction can be seen in the transport phase. In fact, the dominance of transport contribution to the LCOH composition of 2018 is not observed in 2025, where the LCOH is more balanced between each single contribution due to the deployment of the new ships with increased capacity (up to 6.5–11 kton<sub>H2</sub>/shipment) which minimizes the transport cost for all configurations. Also the use of H<sub>2</sub> boil-off in the propulsion system provides further cost reductions in terms of fuel supply (600 ton/shipment, 195 ton<sub>CO2</sub>/shipment), however the fuel cost (0.02 US\$/kg<sub>H2</sub>) is not as impactful as 2018 due to the larger capacity of the ships. For the NH<sub>3</sub> ship the fuel consumption amounts to 0.07 US\$/kg<sub>H2</sub> (1020 ton/shipment equal to 328 ton<sub>CO2</sub>/shipment). The selected demand (15 kton<sub>H2</sub>/year) is probably undersized for the foreseen ship capacities in 2030 (6.5–11 kton<sub>H2</sub>/ship), in fact only 1 ship is used with only 1–3 shipments per year meaning that the ship is not fully exploited to the maximum of its potential.

The import/export port facility storage buffer increases drastically (up to 2300 ton<sub>H2</sub>) due to the larger amounts laden by the new ships. For the LH<sub>2</sub> carrier this entails a relevant increase in cost (around 2 US\$/kg<sub>H2</sub>) while for the NH<sub>3</sub> the increase in cost is only marginal thanks to the carrier characteristics which reduces drastically the specific costs of the storage units.

In general, the Chilean H<sub>2</sub> supply chain pathways are close to the cost target set by METI for 2025, equal to 3 US\$/kg<sub>H2</sub> (CIF – Incoterms 2010). The Chilean trade pathway is

comparable and competitive – especially with the NH<sub>3</sub> carrier – respect to Heuser et. al [15], which report 4.4 US\$/kg<sub>H2</sub> from renewable power in Argentinian Patagonia, which could represent a strategic partner for export H<sub>2</sub> from Latin America to Japan. The final costs are comparable with IEA [8] which indicates a policy target of 3.6 US\$/kg<sub>H2</sub> for H<sub>2</sub> import in Japan and a LCOH range between 5–7 US\$/kg<sub>H2</sub> from Australia, both via LH<sub>2</sub> and ammonia carrier. The LCOH is aligned with import costs from Australia, Norway, Qatar and USA via electrolysis from renewables, ranging between 4.5–5.5 US\$/kg<sub>H2</sub> in 2025 [12]. Other studies, with more detailed modelling [11,31] show more conservative results for renewable hydrogen from Australia, obtaining 6.5–10 US\$/kg<sub>H2</sub> in the same period.

## Conclusions

In this study, a comprehensive techno-economic analysis of the solar H<sub>2</sub> supply chain is performed. The analysis includes H<sub>2</sub> production via ALK and PEM electrolysis supplied by PV and CSP + TES with different energy supply schemes (direct connection and PPA). Subsequently the H<sub>2</sub> is compressed, liquified or stored in an NH<sub>3</sub> carrier to be later transported to Japan, according to the demand set by the guidelines declared by the Japanese government.

In general, the results show that the dependency of the LCOH respect to the balance between specific CAPEX (MUS\$/MW), capacity factor (%) and electricity cost (US\$/MWh) is not straightforward and is affected by country specific characteristics. In the Chilean energy environment, it is more competitive to oversize 2–3 times an electrolyser system coupled with a PV system (25 US\$/MWh – capacity factor around 35%), respect to supplying it with a CSP system (55 US\$/MWh – flat profile) due to the high electricity intensity of the H<sub>2</sub> production process. The lower PV electricity price counterbalances the higher CAPEX of the larger capacity electrolysers coupled to the PV system. PV-fed electrolysis is more cost-competitive supplied by a PPA scheme, while CSP-fed electrolysis the opposite is true, the direct onsite connection is more cost competitive since the increase in electricity cost is more relevant than the marginal increase of the capacity factor. The most cost-competitive production scheme is PV-PPA+ALK reaching 2.20 US\$/kg<sub>H2</sub> (2018) and 1.67 US\$/kg<sub>H2</sub> (2025–2030) with a cost reduction of around 25%. ALK electrolysis results always more cost-competitive respect to PEM although the costs of PEM electrolysis is falling rapidly.

The sensitivity analysis results confirm what can be observed in the LCOH repartition: the impact of cost of electricity and load factor are of paramount importance on the LCOH, by far greater than CAPEX to the point that the system capacity can be oversized up to 2–3 fold before a variation of specific CAPEX reaches the same impact of electricity supply. Water cost is always negligible, even if obtained by seawater desalinization. It must be stated that PV is also much easier to install respect to CSP, due to the technology market maturity gained.

Instead, the H<sub>2</sub> conditioning step is strongly CAPEX-intensive since both the liquefaction; ammonia synthesis



plants are historically designed for steady-state operation. CSP pathways with higher load factors are favoured over PV pathways; hybrid systems achieve the best overall results, allowing to size and operate the conditioning plant with a flat profile while operating on low-cost inlet  $H_2$ . More detailed dynamic simulation of the conditioning plants should be done in order to specifically assess and optimize their performance with variable inputs (part-load operation, flexibility capability, etc.) to determine the actual storage capacity requirement. Increasing storage capacity may affect relevantly the LCOH. Moreover, the storage requirement of the HB unit is more challenging than the liquefaction plant since it depends both on the supply variability and on the flexible operation capability. The latter must be assessed carefully with the available technology in order to obtain realistic cost estimations.

Transport is a relevant cost for 2018 due to the limited capacity of the available ships (170–300 ton $_{H_2}$ /ship) but can be significantly reduced in 2025–2030 thanks to the increase of ship capacity (up to 6.5–11 kton $_{H_2}$ /ship), shifting the most impactful costs on the port storage infrastructure, which increases drastically.

Competitive LCOH values are achieved at the port of arrival for the PV-fed pathways in both 2018 (7.48–7.79 US\$/kg $_{H_2}$  for  $NH_3$  – including reconversion costs – and 9.12–9.34 US\$/kg $_{H_2}$  for  $LH_2$ ) and 2025 (3.94–4.32 US\$/kg $_{H_2}$  for  $NH_3$  – including reconversion costs – and 4.89–5.07 US\$/kg $_{H_2}$  for  $LH_2$ ), respect to METI target prices (10 US\$/kg $_{H_2}$  in 2018 and 3 US\$/kg $_{H_2}$  for 2025) and other strategic pathways identified for the Japanese market.

## Declaration of competing interest

The authors declare that they have no known competing financial interests or personal relationships that could have appeared to influence the work reported in this paper.

## Acknowledgments

H2Chile Chilean Hydrogen Association; Università degli Studi Guglielmo Marconi (DFNSR - Horizon2020 project "BLAZE" Biomass Low cost Advanced Zero Emission small-to-medium scale integrated gasifier-fuel cell combined heat and power plant Grant agreement ID: 815284) & Sapienza University of Rome (DPDTA - Horizon2020 project "GIFT" Geographical Islands Flexibility Grant agreement ID: 824410) are kindly acknowledged for providing financial support for this work.

Hans Kulenkampff from H2Chile is kindly acknowledged for providing feedback regarding electrolyser parameters. Ana María Ruz Frias from Comité Solar is kindly acknowledged to provide guidance for this work.

## REFERENCES

- [1] International Renewable Energy Agency. *Global Renewables Outlook: Energy transformation 2050*. 2020.
- [2] REN21. *Renewables 2019 Global Status Report*. 2019.
- [3] Lew D, Piwko D, Miller N, Jordan G, Clark K, Freeman L. How Do High Levels of Wind and Solar Impact the Grid? The Western Wind and Solar Integration Study. *Energy* 2010;1–10. <https://doi.org/10.2172/1001442>.
- [4] FCH-JU FC and HJU. *Hydrogen Roadmap Europe*. 2019. <https://doi.org/10.2843/249013>.
- [5] Chehade Z, Mansilla C, Lucchese P, Hilliard S, Proost J. Review and analysis of demonstration projects on power-to-X pathways in the world. *Int J Hydrogen Energy* 2019;44:27637–55. <https://doi.org/10.1016/j.ijhydene.2019.08.260>.
- [6] Lefebvre J, Friedemann M, Manuel G, Graf F, Bajohr S, Reimert R, et al. *Renewable Power-to-Gas: A technological and economic review*85; 2016.
- [7] Schiebahn S, Grube T, Robinius M, Tietze V, Kumar B, Stolten D. Power to gas: Technological overview, systems analysis and economic assessment for a case study in Germany. *Int J Hydrogen Energy* 2015;40:4285–94. <https://doi.org/10.1016/j.ijhydene.2015.01.123>.
- [8] IEA International Energy Agency. *The future of fuel: The future of hydrogen*. Report 2019. [https://doi.org/10.1016/S1464-2859\(12\)70027-5](https://doi.org/10.1016/S1464-2859(12)70027-5).
- [9] Reuß M, Grube T, Robinius M, Preuster P, Wasserscheid P, Stolten D. Seasonal storage and alternative carriers: A flexible hydrogen supply chain model. *Appl Energy* 2017;200:290–302. <https://doi.org/10.1016/j.apenergy.2017.05.050>.
- [10] Dagdougui H, Sacile R, Bersani C, Ouammi A. *Hydrogen Storage and Distribution: Implementation Scenarios*. 2018. p. 37–52. <https://doi.org/10.1016/B978-0-12-812036-1.00004-4>.
- [11] Chapman AJ, Fraser T, Itaoka K. Hydrogen import pathway comparison framework incorporating cost and social preference: Case studies from Australia to Japan. *Int J Energy Res* 2017;41:2374–91. <https://doi.org/10.1002/er.3807>.
- [12] ACIL Allen Consulting. *Opportunities for Australia from Hydrogen Exports*. 2018.
- [13] Al-Sharafi A, Sahin AZ, Ayar T, Yilbas BS. Techno-economic analysis and optimization of solar and wind energy systems for power generation and hydrogen production in Saudi Arabia. *Renew Sustain Energy Rev* 2017;69:33–49. <https://doi.org/10.1016/j.rser.2016.11.157>.
- [14] Yang C, Ogden J. Determining the lowest-cost hydrogen delivery mode. *Int J Hydrogen Energy* 2007;32:268–86. <https://doi.org/10.1016/j.ijhydene.2006.05.009>.
- [15] Heuser PM, Ryberg DS, Grube T, Robinius M, Stolten D. Techno-economic analysis of a potential energy trading link between Patagonia and Japan based on CO<sub>2</sub> free hydrogen. *Int J Hydrogen Energy* 2019;44:12733–47. <https://doi.org/10.1016/j.ijhydene.2018.12.156>.
- [16] Dagdougui H. Models, methods and approaches for the planning and design of the future hydrogen supply chain. *Int J Hydrogen Energy* 2012;37:5318–27. <https://doi.org/10.1016/j.ijhydene.2011.08.041>.
- [17] Hydrogen Council. *Path to hydrogen competitiveness A cost perspective*. 2020.
- [18] Sharma S, Ghoshal SK. Hydrogen the future transportation fuel: From production to applications. *Renew Sustain Energy Rev* 2015;43:1151–8. <https://doi.org/10.1016/j.rser.2014.11.093>.
- [19] Morgan E, Manwell J, McGowan J. Wind-powered ammonia fuel production for remote islands: A case study. *Renew Energy* 2014;72:51–61. <https://doi.org/10.1016/j.renene.2014.06.034>.
- [20] Proost J. State-of-the art CAPEX data for water electrolyzers, and their impact on renewable hydrogen price settings. *Int J Hydrogen Energy* 2019;44(9):4406–13. <https://doi.org/10.1016/j.ijhydene.2018.07.164>.

- [21] Schmidt O, Gambhir A, Staffell I, Hawkes A, Nelson J, Few S. Future cost and performance of water electrolysis: An expert elicitation study. *Int J Hydrogen Energy* 2017;42:30470–92. <https://doi.org/10.1016/j.ijhydene.2017.10.045>.
- [22] Element Energy. Hydrogen supply chain evidence base. 2018.
- [23] Reuß M, Grube T, Robinius M, Stolten D. A hydrogen supply chain with spatial resolution: Comparative analysis of infrastructure technologies in Germany. *Appl Energy* 2019;247:438–53. <https://doi.org/10.1016/j.apenergy.2019.04.064>.
- [24] Stolzenburg K, Mubbala R. Integrated Design for Demonstration of Efficient Liquefaction of Hydrogen. *Hydrog Fuel Cells Nord Countries Novemb 1, 2013*. 2013.
- [25] Armijo J, Philibert C. Flexible production of green hydrogen and ammonia from variable solar and wind energy: Case study of Chile and Argentina. *Int J Hydrogen Energy* 2020;45(3):1541–58. <https://doi.org/10.1016/j.ijhydene.2019.11.028>.
- [26] Pacific Northwest National Laboratory. Basic Hydrogen Properties Chart. 2020. <https://h2tools.org/tools>. [Accessed 12 May 2020].
- [27] Cardella U, Decker L, Klein H. Roadmap to economically viable hydrogen liquefaction. *Int J Hydrogen Energy* 2017;42:13329–38. <https://doi.org/10.1016/j.ijhydene.2017.01.068>.
- [28] Ikäheimo J, Kiviluoma J, Weiss R, Holtinen H. Power-to-ammonia in future North European 100 % renewable power and heat system. *Int J Hydrogen Energy* 2018;43:17295–308. <https://doi.org/10.1016/j.ijhydene.2018.06.121>.
- [29] Krewer U, Izzat IC. Operating envelope of Haber – Bosch process design for power-to-ammonia. 2018. p. 34926–36. <https://doi.org/10.1039/c8ra06821f>.
- [30] Hank C, Gelpke S, Schnabl A, White RJ, Full J, Wiebe N, et al. Economics & Carbon Dioxide Avoidance Cost of Methanol Production based on Renewable Hydrogen and recycled Carbon Dioxide – Power-to-Methanol. *Sustain Energy Fuels* 2013. <https://doi.org/10.1039/C8SE00032H>.
- [31] Yoshino Y, Harada E, Inoue K, Yoshimura K, Yamashita S, Hakamada K. Feasibility study of “CO<sub>2</sub> free hydrogen chain” utilizing Australian brown coal linked with CCS. *Energy Procedia* 2012;29:701–9. <https://doi.org/10.1016/j.egypro.2012.09.082>.
- [32] Wold Bank, Solargis, ESMAP. Global Horizontal Irradiation. CHILE: Solar Resource Map; 2020. <https://globalsolaratlas.info/download?c=-17.560244,-71.689455,4>.
- [33] Ministerio de Energía, GIZ. El Potencial Eólico, Solar E Hidroeléctrico De Arica a Chiloé. 2014.
- [34] CEN. Programa Diario de Generación | Coordinador Eléctrico Nacional. 2019. <https://www.coordinador.cl/operacion/graficos/operacion-programada/programa-diario-de-generacion/>.
- [35] Comision Nacional de Energia. Statistical report - Energy 2018. 2018.
- [36] Benavides C, Matus M, Sierra E, Sepúlveda R, Ruz AM, Gallardo F. Value contribution of solar plants to the Chilean electric system. *AIP Conf Proc* 2019;2126. <https://doi.org/10.1063/1.5117671>.
- [37] Gallardo F, Praticò L, Toro C. A thermo-economic assessment of CSP+TES in the north of Chile for current and future grid scenarios. *AIP Conf Proc* 2019;2126. <https://doi.org/10.1063/1.5117535>.
- [38] Ministerio de Energía - Chile. Acta Apertura Ofertas Economicas Licitacion. 2017. 01 n.d.
- [39] Tractebel. Oportunidades para el Desarrollo de una Industria de Hidrógeno Solar en las Regiones de Antofagasta y Atacama: Innovación para un Sistema Energético 100% Renovables. *Com Sol - CORFO*; 2018.
- [40] Ministerio de Energía - Chile. Planificación energética de largo plazo 2019. IAA; 2019. p. 1–80.
- [41] CORFO. Chile's strategy for clean energy and mobility solar energy – lithium – hydrogen. 2017.
- [42] CORFO. Green Hydrogen from Chile. *Innov Week* 2018;7.
- [43] Internationale Zusammenarbeit (GIZ) GmbH, Vásquez R, Salinas F. Tecnologías del Hidrógeno y perspectivas para Chile. *Capítulo* 2018;6:68.
- [44] ENGIE. Renewable Hydrogen. *Renew Hydrog Int Conf* 2018. <https://doi.org/10.1016/B978-0-444-56330-9.00012-7>.
- [45] NEDO. The effort to promote hydrogen in Japan. *Eur Fuel Cell Conf Exhib* 2019. Naples Italy 2019.
- [46] EU-Japan Centre for Industrial Cooperation, Arias J. Hydrogen and Fuel Cells in Japan 1–145; 2019.
- [47] Japanese Ministry of Industry Trade and Economy (METI). Basic Hydrogen Strategy. 2017.
- [48] Kawasaki Heavy Industries. The Hydrogen Road - Paving the Way to a Hydrogen Fueled Future. *KHI Q Newsl* 2015;1–14.
- [49] IRENA. Hydrogen From Renewable Power. 2018.
- [50] Tractebel Engineering and Inicio. Study on Early Business Cases for H<sub>2</sub> in Energy Storage and More Broadly Power To H<sub>2</sub> Applications. 2017. p. 228.
- [51] Yukichi T, Hiroaki K, Ahmer S, Motohiko N. Introduction to a Liquefied Hydrogen Carrier for a Pilot Hydrogen Energy Supply Chain (HESC) project in Japan. *Conf Gastech* 2017. Tokyo n.d.
- [52] ENEA Consulting. The potential of Power-To-Gas. 2016.
- [53] SYSTEMS FIFSE. Photovoltaics Report 2019. 2019.
- [54] DOE Department of Energy. Solar-Plus-Storage 101. *Sol Energy Technol Off* 2019;1–9.
- [55] ENGIE ENERGÍA CHILE S.A.. Presentation to investors Financial update. 2019.
- [56] Bloomberg N. Acciona. Chile Power System Outlook. 2019.
- [57] International Renewable Energy Agency (IRENA). Renewable energy auctions: analysing 2016;1. 2017.
- [58] Palma-Behnke R. The Chilean test system for economic and reliability analysis. In: *IEEE PES Gen Meet PES 2010*; 2010. p. 1–4. <https://doi.org/10.1109/PES.2010.5589718>.
- [59] The World Bank. Electricity Auctions: an overview of efficient practices. *The World Bank*; 2011.
- [60] International Renewable Energy Agency (IRENA). Renewable Power Generation Costs in 2017. 2018.
- [61] Comité Solar, Gallardo Giacomozzi F. Factores críticos en diseño y operación de centrales CSP de torre con almacenamiento en sales fundidas en el desierto de Atacama - Informe de Pasantía. 2017. p. 1–67.
- [62] (MIR) Management Programme in Infrastructure Reform and Regulation, Kruger W, Eberhard A, Swartz K. Renewable Energy Auctions: A Global Overview. 2018.
- [63] International Renewable Energy Agency (IRENA). Renewable Energy Policy Brief: Chile. 2015.
- [64] IEA. Policies - Chile energy auctions. 2019.
- [65] Rudnick H. Risk Responsibility for Supply in Deregulated Electricity Markets - The Chilean Case. 2003. *IEEE Power Eng Soc Gen Meet Conf Proc* 2003;1:525–8. <https://doi.org/10.1109/pes.2003.1267235>.
- [66] Energía CN de. ERNC. Reporte Mensual Noviembre 2019; 2019.
- [67] Coordinador Eléctrico Nacional. Mapa del Sistema Interconectado Central - CDEC SIC. 2020. p. 3–5. <https://sic.coordinador.cl/sobre-sic/sic/>.
- [68] Coordinador Eléctrico Nacional. Información de Instalaciones - Centrales. 2020. p. 1–5. <https://infotecnica.coordinador.cl/instalaciones/centrales>.
- [69] Lopes FM, Conceição R, Silva HG, Fasquelle T, Salgado R, Canhoto P, et al. Short-term forecasts of DNI from an integrated forecasting system (ECMWF) for optimized

- operational strategies of a central receiver system. *Energies* 2019;12:1368.
- [70] JRC European Commission. JRC Photovoltaic Geographical Information System (PVGIS). 2019. [https://re.jrc.ec.europa.eu/pvg\\_tools/en/tools.html#TMY](https://re.jrc.ec.europa.eu/pvg_tools/en/tools.html#TMY).
- [71] Benitez D, Engelhard M, Gallardo F, Jesam A, Kopecek R, Moser M. Technology mix for the Diego de Almagro solar technology district in Chile. *AIP Conf Proc* 2019;2126. <https://doi.org/10.1063/1.5117604>.
- [72] National Renewable Energy Laboratory (NREL). Transparent Cost Database OpenEI; Available Online <https://openei.org/apps/TCDB/>.
- [73] HELIOSCSP. Chile's. 24×7 Concentrated Solar Power Plus Storage Project is Back on Track. 2020. p. 1–6.
- [74] TaiyangNews. Enel Offers Lowest Bid For Chilean Auction. 2017. p. 1–2. <http://taiyangnews.info/MARKETS/ENEL-OFFERS-LOWEST-BID-FOR-CHILEAN-AUCTION/>.
- [75] CleanTechnica. SolarReserve Bids 24-Hour Solar At 6.3 Cents In Chile. *Clean Tech* 2017;1–10. <https://cleantechnica.com/2017/03/13/solarreserve-bids-24-hour-solar-6-3-cents-chile/>.
- [76] SolarPaces. Evening Peak Solar CSP Projected to Undercut Gas in Chile's Open Auctions. 2020. p. 1–21. <https://www.solarpaces.org/evening-peak-solar-csp-projected-to-undercut-gas-in-chiles-open-auctions/>.
- [77] Solarpaces, Kraemer S. SolarReserve Bids CSP Under 5 Cents in Chilean Auction. *Solarpaces* 2017;1–10. <http://www.solarpaces.org/solarreserve-bids-csp-5-cents-chilean-auction/>.
- [78] Gallego B. How to achieve US\$63/MWh in a CSP tower project with storage. *FuturEnergy* 2016;53–5. [www.futureenergyweb.es](http://www.futureenergyweb.es).
- [79] International Renewable Energy Agency (IRENA). *The Power to Change: Solar and Wind Cost Reduction Potential to 2025*. 2016.
- [80] Lilliestam J, Barradi T, Caldes N, Gomez M, Hanger S, Kern J, et al. Policies to keep and expand the option of concentrating solar power for dispatchable renewable electricity. *Energy Policy* 2018;116:193–7. <https://doi.org/10.1016/j.enpol.2018.02.014>.
- [81] Bertuccioli L, Chan A, Hart D, Lehner F, Madden B, Standen Eleanor. Fuel cells and hydrogen Joint undertaking Development of Water Electrolysis in the European Union. 2014.
- [82] Wang M, Wang Z, Gong X, Guo Z. The intensification technologies to water electrolysis for hydrogen production - A review. *Renew Sustain Energy Rev* 2014;29:573–88. <https://doi.org/10.1016/j.rser.2013.08.090>.
- [83] Buttler A, Spliethoff H. Current status of water electrolysis for energy storage, grid balancing and sector coupling via power-to-gas and power-to-liquids: A review. *Renew Sustain Energy Rev* 2018;82:2440–54. <https://doi.org/10.1016/j.rser.2017.09.003>.
- [84] FCH-JU FC and HJU. Study on hydrogen from Renewable Resources in the EU. Fuel Cells Hydrog Jt Undert (FCH JU) Final. Rep 2015. <https://doi.org/10.1007/s13398-014-0173-7.2.XXXIII>.
- [85] Felgenhauer M, Hamacher T. State-of-the-art of commercial electrolyzers and on-site hydrogen generation for logistic vehicles in South Carolina. *Int J Hydrogen Energy* 2015;40:2084–90. <https://doi.org/10.1016/j.ijhydene.2014.12.043>.
- [86] Eypasch M, Schimpe M, Kanwar A, Hartmann T, Herzog S, Frank T, et al. Model-based techno-economic evaluation of an electricity storage system based on Liquid Organic Hydrogen Carriers. *Appl Energy* 2017;185:320–30. <https://doi.org/10.1016/j.apenergy.2016.10.068>.
- [87] Lokke JA. Nel Group 2017.
- [88] Molinos-Senante M, Donoso G. Water scarcity and affordability in urban water pricing: A case study of Chile. *Util Policy* 2016;43:107–16. <https://doi.org/10.1016/j.jup.2016.04.014>.
- [89] Campero C, Harris LM. The legal geographies of water claims: Seawater desalination in mining regions in Chile. *Water (Switzerland)* 2019;11:1–21. <https://doi.org/10.3390/w11050886>.
- [90] IEA International Energy Agency. *IEA G20 Hydrogen report : Assumptions*. 2019.
- [91] DOE. *Hydrogen Delivery. Fuel Cell Technol Off Multi-Year Res Dev Demonstr Plant*; 2015. p. 37–54.
- [92] Fuhrmann J, Hülsebrock M, Krewer U. *Energy Storage Based on Electrochemical Conversion of Ammonia*. 2013.
- [93] Liu H. Ammonia synthesis catalyst 100 years : Practice , enlightenment and challenge. *Chinese J Catal* 2014;35:1619–40. [https://doi.org/10.1016/S1872-2067\(14\)60118-2](https://doi.org/10.1016/S1872-2067(14)60118-2).
- [94] Kandemir T, Schuster ME, Senyshyn A, Behrens M, Schlögl R. The Haber – Bosch Process Revisited : On the Real Structure and Stability of “ Ammonia Iron ” under Working Conditions \*\*. *Angewandte* 2013;12723–6. <https://doi.org/10.1002/anie.201305812>.
- [95] Fertilizers Europe. *Best Available Techniques (BAT) for Pollution Prevention and Control in the European Fertilizer Industry*. 2000.
- [96] Tuna P, Hultberg C, Ahlgren S. Techno-Economic Assessment of Nonfossil Ammonia Production 2014;33. <https://doi.org/10.1002/ep>.
- [97] Tremel A, Wasserscheid P, Baldauf M, Hammer T. Techno-economic analysis for the synthesis of liquid and gaseous fuels based on hydrogen production via electrolysis. *Int J Hydrogen Energy* 2015;40(35):11457–64. <https://doi.org/10.1016/j.ijhydene.2015.01.097>.
- [98] Union IG. *Small scale LNG*, 2; 2015.
- [99] Bialystocki N, Konovessis D. On the estimation of ship's fuel consumption and speed curve: A statistical approach. *J Ocean Eng Sci* 2016;1:157–66. <https://doi.org/10.1016/j.joes.2016.02.001>.
- [100] Ship, Bunker. *Average Bunker Prices. Sh Bunker*; 2017. <https://shipandbunker.com/prices/av>.
- [101] World LPG Association. *Guide for LPG Marine Fuel Supply*. 2019.
- [102] ISGAS Energit Multiutilities S.p.A. *Terminal GNL nel Porto Canale di Cagliari - Progetto Autorizzativo*. 2019.
- [103] EPA. In: *Emission Factors for Greenhouse Gas Inventories*, 40; 2017. <https://doi.org/10.1177/0160017615614897>.
- [104] Statista. *Energy sector in Japan - Statistics & Facts*. 2020.
- [105] Morgan ER. *Techno-Economic Feasibility Study of Ammonia Plants Powered by Offshore Wind*. Univ Massachusetts - Amherst, PhD Diss; 2013. p. 432.

## List of Acronyms

ALK: Alkaline  
 CAPEX: Capital Expense  
 CFR: Cost & Freight (Incoterms 2010)  
 CGH<sub>2</sub>: Compressed Gaseous Hydrogen  
 CL: Chile  
 CSP: Concentrated Solar Power  
 HB: Haber-Bosch  
 JP: Japan  
 LCOA: Levelised Cost Of Ammonia  
 LCOH: Levelised Cost Of Hydrogen  
 LH<sub>2</sub>: Liquified Hydrogen  
 LHV: Lower Heating Value  
 NG: Natural Gas  
 O&M: Operation & Maintenance

LNG: Liquefied Natural Gas  
OPEX: Operating Expense  
PEM: Proton Exchange Membrane or Polymer Electrolyte Membrane  
PPA: Power Purchase Agreement  
PV: Photovoltaic  
RES: Renewable Energy Sources  
SEC: Specific Energy Consumption  
SMR: Steam Methane Reforming  
TES: Thermal Energy Storage  
TMY: Typical Meteorological Year  
WACC: Weighted Average Cost of Capital

#### Notations & Symbols

$\beta$ : pressure ratio  
 $\eta$ : efficiency  
 $c_p$ : specific heat coefficient (constant pressure)

$c_{sp}$ : specific energy consumption  
 $k$ : heat capacity ratio  
 $m$ : mass  
 $\dot{m}$ : mass flow  
 $P$ : power  
 $T$ : temperature  
 $\Delta T$ : temperature difference

#### Subscripts

1: input compressor  
2: output compressor  
AC: alternate current  
 $e$ : electrical  
 $el$ : electrolyser  
 $H_2$ : hydrogen  
 $m$ : mechanical  
 $nom$ : nominal